



REFERENCE STUDY REPORT

No 78 (1998)

RACKING RESISTANCE OF BRACING WALLS IN LOW-RISE BUILDINGS SUBJECT TO EARTHQUAKE ATTACK

Volume 2

Experimental Program Derivation & Assessment

P.D. Herbert and A.B. King

This is the second of two volumes which combine to report on how wall bracing panels which develop slackness can rationally be used as a structural system to resist earthquakes. A summary of findings and a proposed revision to the current P21 test method and related references are contained in Volume 1. Volume 2 focuses on the experimental programme which underpins the recommended changes. It is intended that the combined report will be used by technical advisers to building product manufacturers seeking to use their product as wall bracing elements within New Zealand houses. It provides the engineering rationale upon which a revision of the Wall Bracing Test and Evaluation Method known as the BRANZ P21 test method is proposed. As such it is also intended for use by Building Control Authorities and Structural Engineers can utilise the bracing ratings derived for specific engineering design.

PREFACE

This volume contains the experimental results for the project. The completed experimental programme was undertaken in three phases, each of which is covered separately within this volume. In all cases the behaviour of timber framed bracing panels under wind or earthquake racking is examined with a view to addressing anomalies such as the degree of end restraint and the onset of premature brittle failure associated with lining degradation. The findings from this experimental programme are used to support the proposed revision to the test and evaluation method contained in Volume 1.

ACKNOWLEDGMENTS

The authors acknowledge financial support for this study from the Building Research Levy, the Public Good Science Fund of the Foundation for Research, Science and Technology and the Earthquake Commission Research Foundation. The authors wish to thank Winstone Wallboards Ltd and James Hardie and Co Pty Ltd for providing materials for this project.

RACKING RESISTANCE OF BRACING WALLS IN LOW-RISE BUILDINGS SUBJECT TO EARTHQUAKE ATTACK

BRANZ Study Report SR 78

P.D.Herbert and A.B.King

Reference

Herbert, P.D and King, A.B. 1998. Report on Racking Resistance Test and Evaluation Procedure. Building Research Association of New Zealand, Study Report SR 78, Judgeford, New Zealand.

Herbert, P.D and King, A.B. 1997. Report on Racking Resistance Test and Evaluation Procedure. Building Research Association of New Zealand, Study Report SR 78, Judgeford, Wellington, New Zealand.

Abstract

Lateral loads such as those produced by the effects of wind and earthquake can be resisted in buildings by cantilever action, by moment resisting frames, by shear walls, by diagonal bracing or a combination of these.

In New Zealand light timber frame construction, the resistance is provided entirely by shear walls. The total resistance of a wall is determined by summing the dependable strengths of individual full height panels located between openings. The standard method for assessing the racking resistance of wall bracing elements between openings, since 1978, has been the BRANZ P21 test. It has been known for some time that there are deficiencies with the P21 test and evaluation procedure with major problems being whether the test loading regime can adequately identify severely degrading elements, and in the assessment of wall ductility.

A detailed literature survey of wall racking tests carried out around the world and the factors which contribute to bracing panel behaviour is given. Taking this into account, a three phase experimental programme was carried out on bracing panels under various loading protocols, including monotonic and reverse cyclic loading. The end studs to the specimens were either fully held down with tie-rods, or restrained from uplift by the application of a vertical load or use of a partial restraint. A series of experiments was also carried out with no restraint to the end studs. The test specimens were lined with sheathings commonly found in New Zealand construction.

Both the onset of damage to the panels and the displacements at which a significant drop off in load occurred were investigated.

Methodology is presented in this report to enable an accurate computer model to be matched to the test element response. Once matched, the model may then be used to analyse the performance of the element under dynamic seismic loading and to generate seismic response spectra. The result from this analysis is quantification of the mass that the test panel can dependably restrain without the necessity to assess wall ductility.

CONTENTS

	Page No.
1. EXPERIMENTAL PROGRAMME PHASE I	1
1.1 Objective.....	1
1.2 Description of Test Specimens.....	1
<i>1.2.1 End stud uplift Restraints used</i>	4
1.3 Phase I Experimental set-up	7
1.4 Phase I Experimental Procedure	7
1.5 Phase I Experimental Observations	8
<i>1.5.1 General</i>	8
<i>1.5.2 Monotonic Displacement Protocol with P21 Uplift Restraints</i>	8
<i>1.5.3 Cyclic Load and Displacement Protocols with P21 End Restraints</i>	11
<i>1.5.4 Cyclic Load and Cyclic Displacement Test Regime Using Various End Restraints</i>	15
<i>1.5.5 Panel W17 (Lintel Specimen)</i>	18
<i>1.5.6 Description of Light Timber Frame Bracing Panel Hysteretic Behaviour</i>	20
1.6 Conclusions to Experimental Programme Phase I	21
2. EXPERIMENTAL PROGRAMME PHASE II	21
2.1 Objective.....	22
2.2 Description of Test Specimens	22
2.3 Displacement Protocol.....	23
2.4 Observations	23
<i>2.4.1 General</i>	23
<i>2.4.2 Panel W18 - BL with P21 Restraint</i>	23
<i>2.4.3 Panel W19 - BL with Tie Down Rod Restraint</i>	24
<i>2.4.4 Panel W20 - PY with P21 Restraint</i>	24
<i>2.4.5 Panel W21 - PY with Tie Down Rod Restraint</i>	25
<i>2.4.6 Panel W22 - PB + BL with end Straps. P21 Restraint</i>	26
<i>2.4.7 Panel W23 - PB Both Sides with P21 Restraint One End and Minimal Restraint the Other</i>	28
<i>2.4.8 Panel W24 -PB Both Sides with P21 Restraint One End and 12 kN Restraint the Other</i>	29
2.5 Summary of Performance Evaluation of Phase II Systems	30
2.6 Comparison of Individual Test Panel Results with Previous Work.....	31
2.7 Conclusions From the Phase II Experimental Programme.....	32
3. EVALUATION PROCEDURE USED TO DETERMINE THE DEPENDABLE SEISMIC MASS RESTRAINED.	33

	Page No.
3.1	Introduction 33
3.2	Seismic Mass Rating Procedure 34
3.3	Results of Phylmas Analysis for Test Programme I 35
3.3.1	<i>P21 Restraint</i> 35
3.3.2	<i>NZA Earthquake Record - A Comparison of Spectra</i> 36
3.3.3	<i>Displacement and Acceleration spectra using various restraints</i> 37
3.3.4	<i>Panel W16 - BL Lined Both Sides, Tie Down Rod Restraint</i> 38
3.3.5	<i>Panel W17 - Lintel Specimen</i> 38
4.	DISCUSSION 39
4.1	Boundary Conditions 39
4.1.1	<i>Uplift Restraint Attributable to Current P21 (1991) End Restraint</i> 40
4.2	In-service Boundary Conditions. 41
4.2.1	<i>Internal Bracing Panel / External Wall Junction</i> 41
4.2.2	<i>Internal Bracing Panel / Door Opening</i> 43
4.3	Load Regime..... 43
4.3.1	<i>Load or Displacement Control</i> 44
5.	CONCLUSION 45
6.	REFERENCES 46
7.	APPENDIX A SMALL SCALE TESTING OF BRACING PANEL COMPONENTS 48
8.	APPENDIX B BRACING PANEL UPLIFT ON TYPICAL TIMBER FLOORING 49

FIGURE	Page No.
Figure 1 : Typical Test Set-Up	3
Figure 2 : Panel W17 Configuration.....	3
Figure 3 : P21 End Restraint	4
Figure 4 : Test Specimen with Tie-Rod Restraint	5
Figure 5 : Test Specimen with Vertical Load.....	6
Figure 6 : Load Displacement Response for Specimens subjected to Monotonic Displacement Protocol	10
Figure 7 : Cyclic and Monotonic Load Regime for 2.4m long panels with different linings.....	12
Figure 8 : Percentage Load Degradation from Monotonic Curve (BL) Specimens W10 and W12.....	13
Figure 9 : Displacement at Successive Cycles as a Ratio of Peak Load.....	14
Figure 10: Hysteresis Loops for Panel W13 - Specimen with Tie-Down Rod Restraint ...	16
Figure 11: Hysteresis Plot for Specimen W14 - Vertically Loaded Top Plate	17
Figure 12: Predicted Monotonic Parent Curves - Panel W17	19
Figure 13: Hysteresis plots for Specimens W18-W23	27
Figure 14: Hysteresis Loop for Specimen W24.....	29
Figure 15: Comparison of Parent Curves for Lintel and Long Walls.....	31
Figure 16: Displacement Spectra Specimen W12	35
Figure 17: Mass Restrained using Various End Restraints	38
Figure 18: Mass Restrained by Specimens W13 and W16.....	39
Figure 19: Typical Wall Junction	42
Figure 20: Parent Curves Under Load or Displacement Control	45

TABLE

Table 1 : Test Specimen Configurations	2
Table 2: Specimen Cyclic Test Regime - Load Control.....	7
Table 3: Specimen Cyclic Test Regime - Displacement Control.....	8
Table 4: Ratio of Displacement to Residual Displacement.....	14
Table 5: Test Specimen Configuration.....	22
Table 6: Test Load Regime for Test programme II.....	23
Table 7: Restrained Masses for Specimens W18-W24	30
Table 8: Comparison of Restrained Mass for Long Wall Panel.....	32
Table 9: Comparison of Mass Restrained using P21 End Restraint	36
Table 10: Comparison of Mass Restrained using Various End Restraints	37
Table 11: Lateral Force per Bottom Plate Fixing.....	41

1. EXPERIMENTAL PROGRAMME PHASE I

1.1 Objective

The first phase of the experimental programme was designed to:

- Determine a load/displacement protocol which enables the onset of damage of bracing panels to be identified.
- Determine the effect that the alternatives of either load or displacement control had, if any, on the peak resistance of the bracing systems.
- Determine the effect that different boundary conditions (ie end stud uplift restraints and also the degree of sill plate fixity) had on panel strength and stiffness.
- Determine the amount of restraint afforded by lintels.
- Provide data to verify the Phylmas computer programme. Details of the programme can be found in Section 3.

1.2 Description of Test Specimens

All frames were constructed from machine stress graded 90 x 35 mm kiln dried radiata pine studs and 90 x 45 mm kiln dried radiata pine top and bottom plates and machine stress graded to grade F5. All frames, except for panel W17 described below, were 2420 mm high and 2435 mm long. Frame studs were centred at 600 mm nailed together using two 90 x 3.15 mm gun nails. Panels W4-W6 had one row of noggins at mid height. All other panels were devoid of noggins.

Bottom plates to panels W1-W16 were nailed to a 150 x 90 timber foundation beam, through a 20 mm particleboard strip, using pairs of 100 x 4 mm flat head nails at 600 mm centres. The particleboard strip represents typical flooring. The foundation beam was bolted rigidly to a purpose built steel framed test rig. The typical test set-up is shown in Figure 1.

Panel W17 was uniquely constructed to simulate a short section of wall between two door openings. The bottom plate of the panel was fixed to a 300 x 100 mm timber foundation beam using pairs of 100 x 4 mm flat head nails at 600 mm centres. The foundation beam was firmly bolted to the laboratory strong floor and had a 20 mm strip of particleboard fixed to its upper face. The door lintels were constructed using 90 x 35 mm F5 kiln dried radiata pine and were checked 15 mm into the studs. The top plate was continuous. Hold down restraints were provided at the extreme ends of the specimen by means of 16 mm diameter tension rods clamped to the lintel and fixed directly to the strong floor. This prevented uplift at the tension end of the panel during load cycling but did not prevent vertical downward movement of the end stud in compression. Ten kN load cells were used to measure the uplift in the restraining rods. (see Figure 2).

Various linings were used in the tests. Linings were used on one side only, with the exception of panels W16 and W17 which were lined both sides. All linings were fixed using galvanised clouts.

Variations in the lining material, the end boundary restraint and the loading regime are identified in Table 1 below.

Panel	Lining	Restraint	Load Regime
W1	PB	P21	Monotonic
W2	PB	P21	Cyclic/Load Control
W3	PB	P21	Cyclic/Disp Control
W4	FC	P21	Monotonic
W5	FC	P21	Cyclic/Load Control
W6	FC	P21	Cyclic/Disp Control
W7	PY	P21	Monotonic
W8	PY	P21	Cyclic/Load Control
W9	PY	P21	Cyclic/Disp Control
W10	BL	P21	Monotonic
W11	BL	P21	Cyclic/Load
W12	BL	P21	Cyclic/Disp Control
W13	BL	Tie Rod	Cyclic/Load Control
W14	BL	Vert Load	Cyclic/Load Control
W15	BL	None	Cyclic/Load Control
W16 ¹	BL	Tie Rod	Cyclic/Load Control
W17 ^{1,2}	PB	Refer Figure 2	Cyclic/Disp

Table 1 : Test Specimen Configurations

¹ Lined both sides

² Lintel Specimen. Refer Figure 2

The four proprietary linings used were:

PB - Nominal 9.5 mm standard grade paper faced plasterboard¹ fixed with 30 x 2.5 galvanised clouts at 150 mm c/c to panel perimeter. 300 mm c/c at lining join and pairs of clouts at 300 mm c/c on intermediate studs.

FC - Nominal 7.5 mm thick smooth faced fibre cement sheet², fixed with 40 x 2.5 galvanised clouts at 150 mm c/c to panel perimeter, internal studs and noggins.

PY - Nominal 7.5 mm thick plywood sheet with three laminates, measured thickness was 7.8 mm and density 4.1 kg/m² fixed with 30 x 2.5 galvanised clouts at 150 mm c/c to sheet edges and at 300 mm c/c to intermediate studs.

BL - Nominal 9.5 mm enhanced paper faced bracing plasterboard³ fixed as per the plasterboard pattern above but with purpose made washers beneath the nails around the panel perimeter.

¹ Winstone Wallboards Ltd standard Gib® plasterboard of measured thickness of 9.5 mm and density 6.7 kg/m².

² James Hardie Harditex® with a measured thickness of 7.6 mm and density 10.3 kg/m².

³ Winstone Wallboards Ltd Gib® Braceline with a measured thickness of 9.5 mm and density 8.46 kg/m².

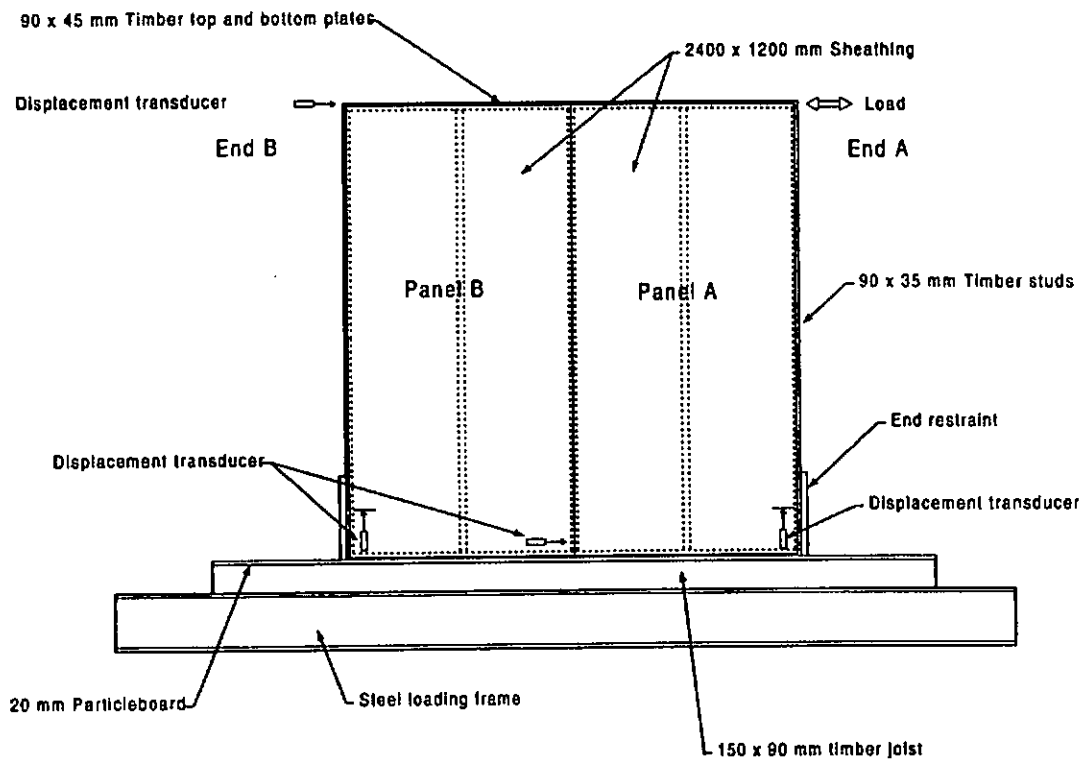


Figure 1 : Typical Test Set-Up

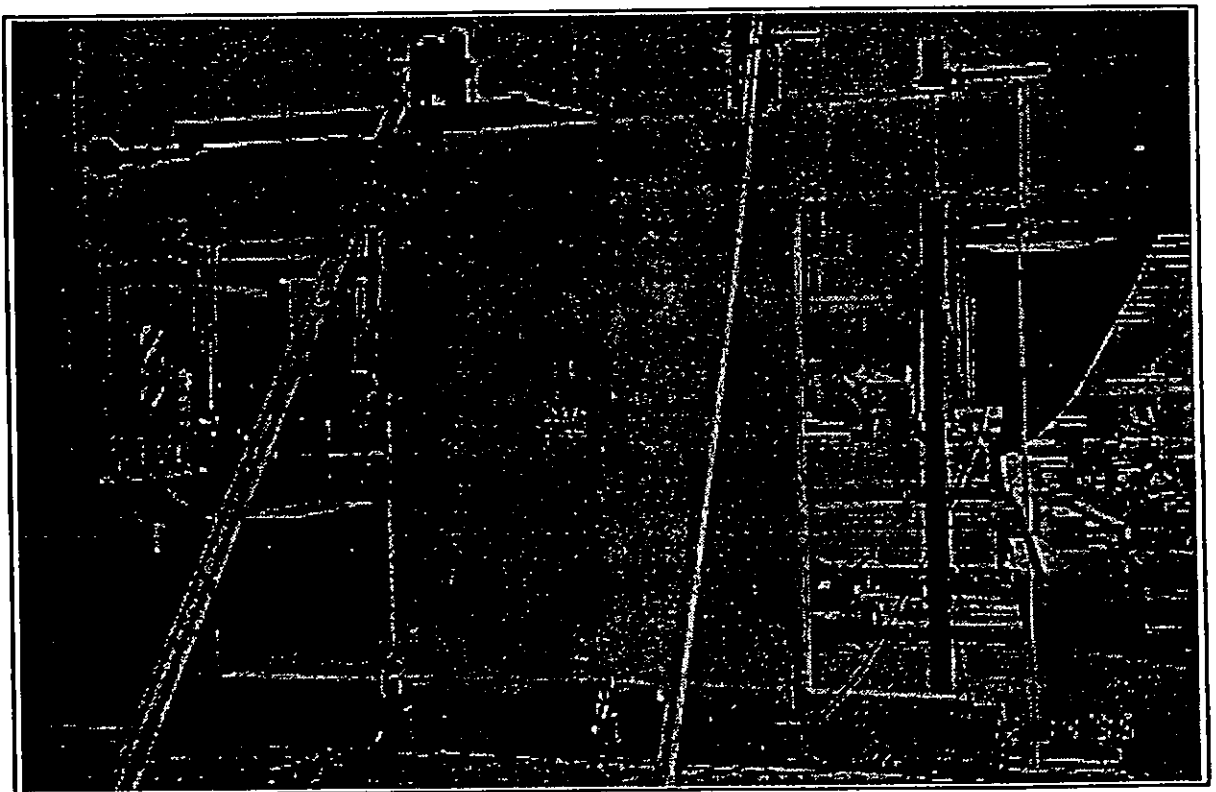


Figure 2 : Panel W17 Configuration

Both sides of the panel were lined with 9.5 mm plasterboard, with joints fully stopped and taped. A 25 x 1 mm (nominal) galvanised high tensile steel strap was used to form a diagonal brace within the main body of the specimen.

The panel was similar to a section of wall tested by Thurston (1993) so observations and results from each of the tests could be readily compared.

1.2.1 End stud uplift restraints used

The effect of varying degrees of uplift restraint were investigated in panels W1 to W16. Four levels of restraint were imposed as follows:

- i) **P21 Restraint** - Consisting of a portion of stud fixed to each end of the test specimen using three No. 100 x 4 mm flat head nails fixed horizontally. The stud portion was restrained from uplifting by bearing against a mild steel angle which was bolted down to the test rig. Refer Figure 3. Reference to the P21 restraint is made throughout this document and refers to this detail.

This method of restraint is the one currently employed for the BRANZ P21 test method (King & Lim 1991) and is considered as representative of the minimum restraint afforded by the intersection of cross walls at bracing panel ends.

- ii) **Tie Rods** - Four 16 mm diameter mild steel rods were placed in pairs at each end of the specimen. The rods extended the full height of the specimen and bolted rigidly at the bottom to the test rig. The top of the rods were bolted and hand tightened to a mild steel angle which was placed across the specimens over the end stud. The mild steel angle was mounted onto a load skate to allow the specimen to move horizontally without restraint. Refer Figure 4.

The vertical restraint provided a full tie down and prevented specimen rigid body rotation. It is an adaptation of the method used in ASTM E72 (ASTM 1976) as described in Vol I section C.1.2

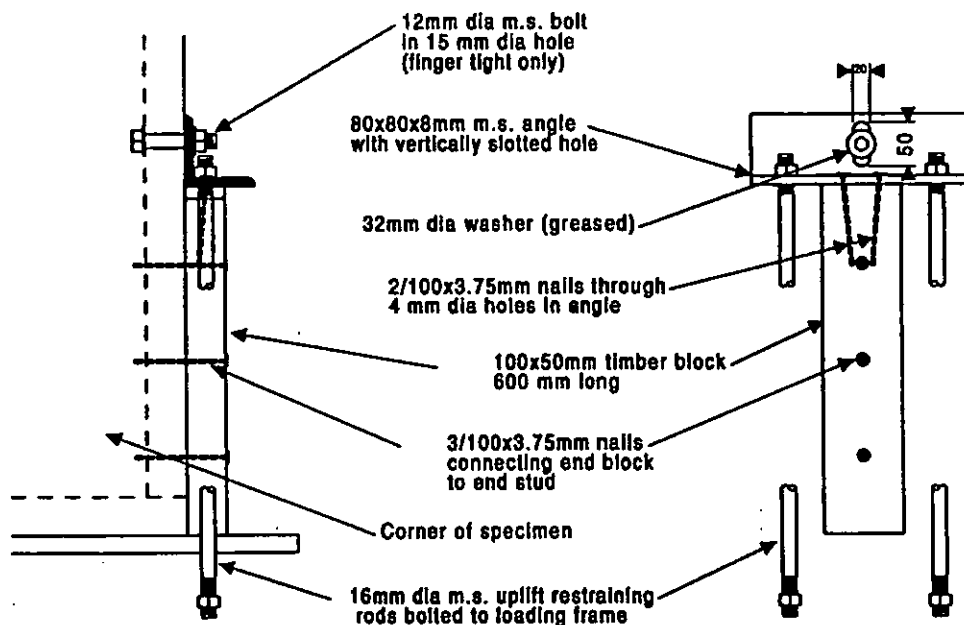


Figure 3: P21 End Restraint

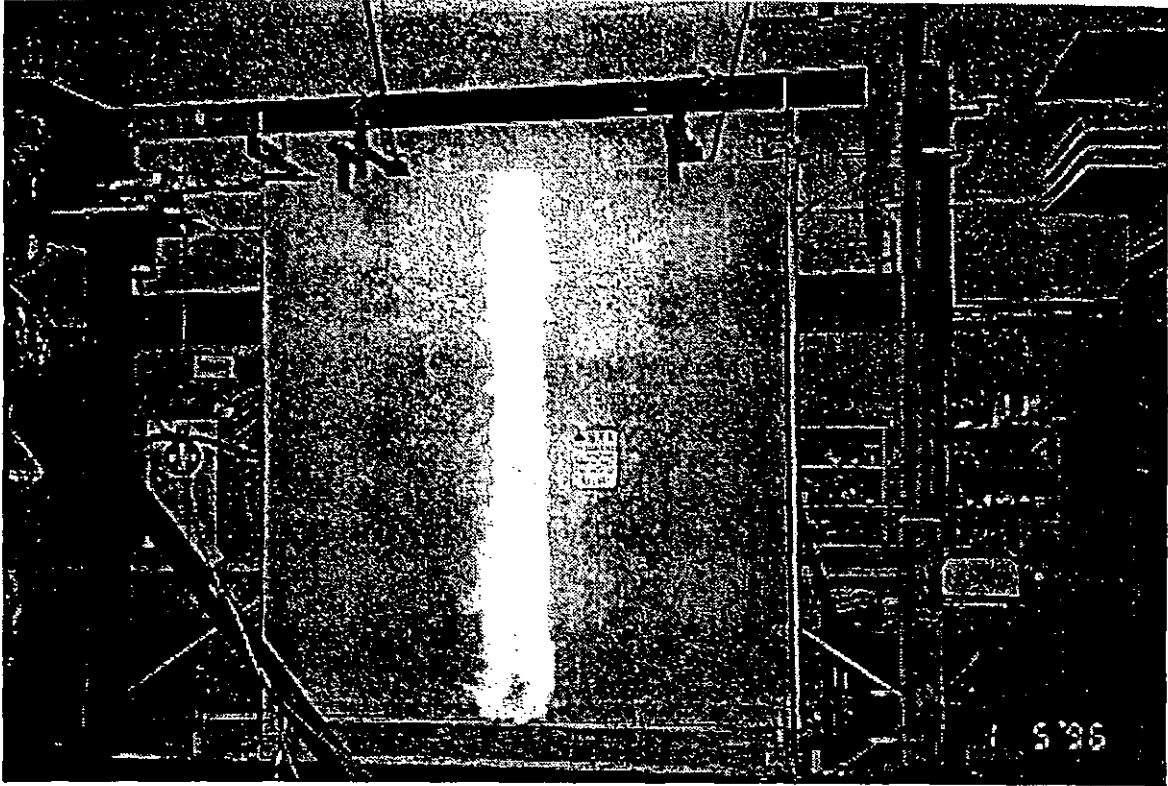


Figure 4 : Test Specimen with Tie-Rod Restraint

- iii) **Vertical load** - A vertical load was applied to specimen W14 by means of two 125 kg weights suspended from the end of a cross piece bearing onto the top plate. The other end of the cross piece was tied down to the test rig using a 16 mm tie rod. Refer Figure 5. The resultant vertical load imposed through the lever arm of the cross piece was equivalent to a vertical mass of 1000 kg. No other restraints were used.

The load represented a lower storey panel carrying 8 m width of lightweight roof and 3m width of floor. The load was transferred to the studs via a steel spreader beam which was packed off the top plate at the stud positions.

- iv) **No restraint** - This test was carried out without any additional restraints or gravity loads.

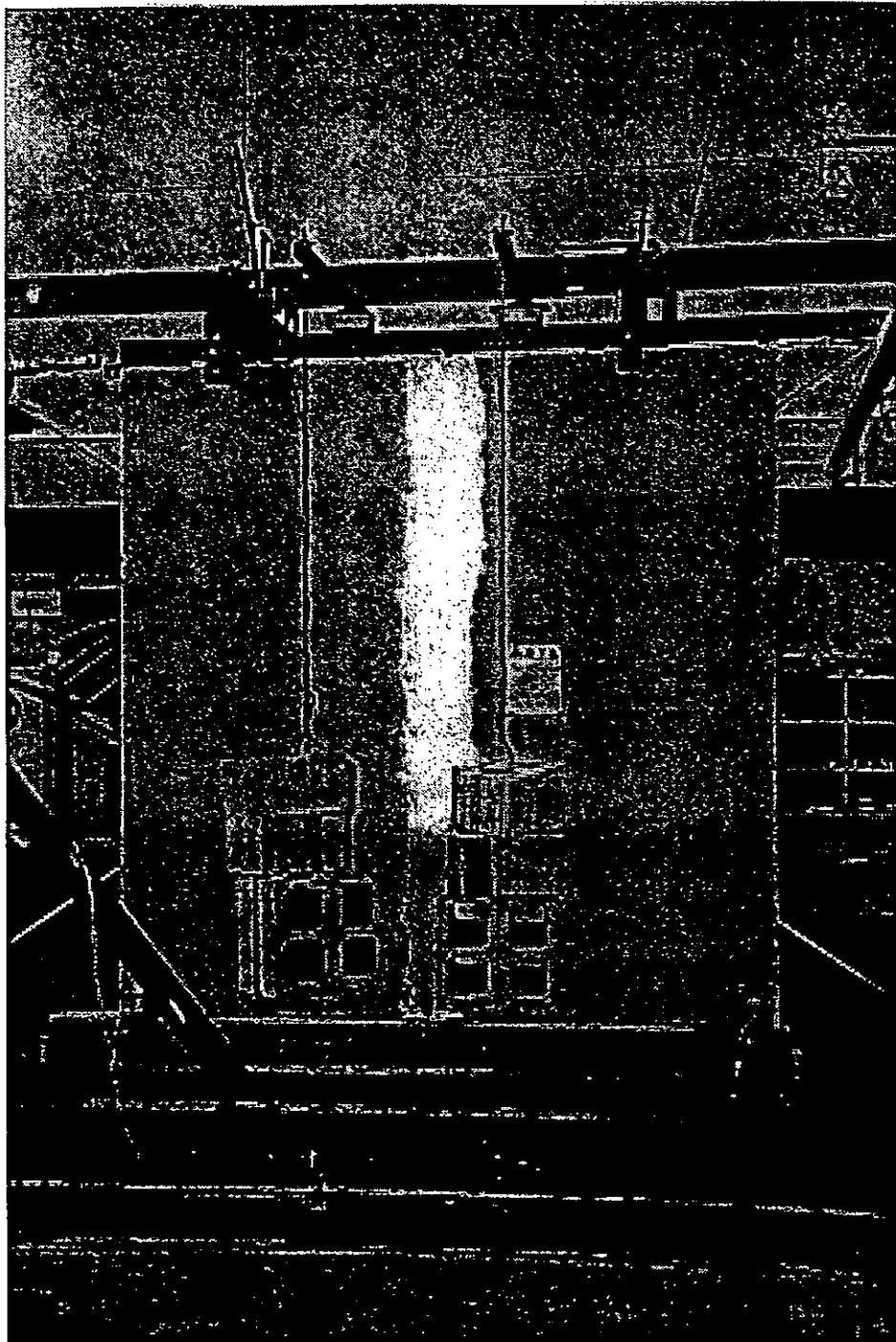


Figure 5: Test Specimen with Vertical Load

1.3 Phase 1 Experimental set-up

Panels W1-W16 were tested in a vertical orientation in a rigid steel loading frame. Horizontal load was applied to the specimen top plate with a 30 kN closed loop electro-hydraulic ram and measured with a 20 kN load cell.

Panel W17 was tested on the strong floor with the horizontal load applied with a 90 kN closed loop electro-hydraulic ram reacting against a strong wall and measured with a 100 kN load cell. A linked pair of steel channels was screwed to the top plate, (but not over the lintels) which transferred the horizontal load to the panel.

Steel rollers were used to prevent out of plane movement of the top plate. Load cells were selected such that they were accurate to within 1% at the peak loads encountered. Linear potentiometers, reading to an accuracy of 0.1mm, were used to measure:

- horizontal deflections of the top and bottom plates
- vertical uplift of the studs at either end of the specimen
- lining slip relative to the frame.

Test load and displacement measurements were recorded using an IBM compatible PC running a proprietary software programme to record the data.

1.4 Phase 1 Experimental Procedure

Three load/displacement protocols were used:

- Monotonic* - Horizontal load was applied to the top plate at an approximately constant rate of 5 kN/min in one direction only. The specimen was pushed until failure.
- Cyclic / Load Control* - The maximum load reached during the monotonic test (i) above, was noted and used as the basis of controlling the loading cycle. The basic cyclic test regime is shown in Table 2.

Load/kN	No. of Cycles
$\pm 0.5 P_u^*$	3
$\pm 0.6 P_u$	3
$\pm 0.8 P_u$	3
$\pm 0.9 P_u$	3
$\pm 1.0 P_u$	3

Table 2. Specimen Cyclic Test Regime - Load Control

* P_u = Peak load recorded in Monotonic Test.

- iii) *Cyclic / Displacement Control* - The displacement Δu reached at the Peak load P_u during the monotonic test was used as the basis of controlling the displacement cycles. Refer Table 3.

Displacement	No. of Cycles
$\pm 0.6 \Delta_u$	3
$\pm 0.8 \Delta_u$	3
$\pm 0.9 \Delta_u$	3
$\pm 1.0 \Delta_u$	3
$\pm 1.1 \Delta_u$	3

Table 3 : Specimen Cyclic Test Regime - Displacement Control

1.5 Phase 1 Experimental Observations

1.5.1 General

The lining commonly experienced local distortions at the fastener as the imposed displacement increased. The zone of greatest distortion was generally along the bottom plate, particularly at the extreme corners during initial cycles, but progressing along the full extent of the bottom plate and eventually along each end stud.

In the following section the terms “nails working” or “working hard” (when distortions were more severe) are used to describe the observation that the nail heads were embedding into the lining material. If a nail head pulled through the sheet, this is referred to as “nail head pull through”.

The following observations were made at the corresponding horizontal top plate displacements. Observations for specimens subjected to cyclic loading under both load and displacement control were similar and have been grouped together under the one heading. The general description of displacement relates to the horizontal top plate displacement.

The ends of the specimen described as end A or B are shown in Figure 1.

1.5.2. Monotonic Displacement Protocol with P21 Uplift Restraints

1.5.2.1 *PB - Specimen W1 (see also Figure 6)*

@ Displacement mm	Observations
10	Bottom corner nails were ‘working hard’, with the remainder of bottom plate fixings “working”.
15	Damage increased and top plate nails were observed to be ‘working’. Bottom corner fixings had ‘pulled through’. This coincided with the maximum resistance.
15-30	Resistance reasonably constant
30	All nails to bottom plate and some of the top plate fixings had ‘pulled through’. Large load drop off. Very little uplift of the end studs was observed.

1.5.2.2 FC Specimen W4 (see also Figure 6)

@ Displacement mm	Observations
20	Generally, the lining experienced little damage throughout the test. 'Twisting' of the bottom plate occurred at displacements greater than 20 mm.
30	Bottom plate fixings to foundation at end A almost totally withdrawn. (ie had lifted some 50 mm).
55	At 55 mm displacement the three nails of the P21 restraint were severely bent. The lining however remained largely undamaged.

1.5.2.3 PY Specimen W7 (see also Figure 6)

@ Displacement mm	Observations
15	Fixings began to 'work' along the bottom plate.
18	The tension end stud uplifted from bottom plate approximately 4 mm, equalling the uplift observed between the bottom plate and the foundation.
30	Peak Load recorded
45	Fixings to the lining/bottom plate continued to 'work hard', with nails at both end studs beginning to 'work'.
70	The two plywood sheets were rotating independently of one another. There was little drop off in resistance from the peak at 30 mm, to displacements in excess of 70 mm.

1.5.2.4 BL Specimen W10 (see also Figure 6)

@ Displacement mm	Observations
15	Bottom plate fixings were 'working slightly', and the bottom plate began to lift off the foundation beam. There was no apparent separation of the end stud from the bottom plate.
15-26	Resistance increased with the fixings 'working hard'.
26	The bottom extreme corner fixings were pulled through.
40	Little increase in load but the fixings at the bottom of the end stud began to 'pull through' at each end. The bottom plate was observed to be 'twisting' with the lined side pulling up higher than the unlined side. There was a drop off in load at this point.
55	The fixings down the centre joint between sheets were 'working hard'.
70	The tension end stud was observed lifting from the bottom plate approx 10 mm, and the same distance was noted between bottom plate and foundation. The top plate had separated from the end stud at end A by some 30 mm.

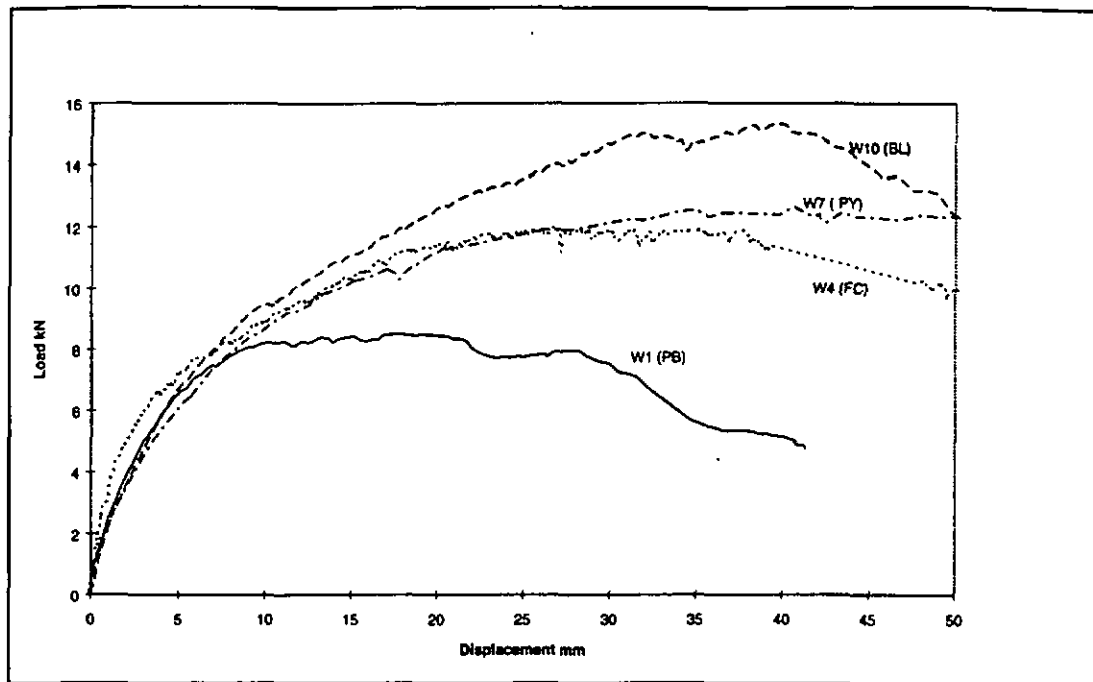


Figure 6 : Load Displacement Response for Specimens subjected to Monotonic Displacement Protocol

The initial stiffnesses (up to 4 kN) are similar, approximately 1.7 kN/mm with the exception of the fibre cement lining which had an initial stiffness of ≈ 3.3 kN/mm.

The plasterboard specimen (W1) attained a peak load of approximately 8 kN at which time there was a marked stiffness degradation. The panel was able to sustain this load over a wide displacement range; up to around 30 mm when there was a drop off in load carrying capability. The stiffness degradation for the other panels was not as severe as W1 and they were able to attain peak loads 50% higher. (Around 12 kN for both W4 and W7 and 14 kN for panel W10).

At the end of the test on panel W10 it was found that the bolts used to secure the angle restraint were very tight, normally they would be only tightened by hand. This may have led to the specimen being over-restrained and hence the higher peak load values. Previous tests carried out indicate that the monotonic curve would usually be similar to those obtained for fibre cement board or plywood because the hold-down strength usually limits the strength of the panel.

In all cases, the panels were able to sustain their load carrying capabilities during large inelastic deformations.

1.5.3. Cyclic Load and Displacement Protocols with P21 End Restraints

1.5.3.1 *PB Specimens W2 & W3 (see also Figure 7)*

@ Displacement mm	Observations
5	The bottom corner fixings were seen to be 'working'. There was little increase in displacement recorded prior to the bottom corner of the sheet fracturing. As displacements increased the top plate fixings began to work.
11	Complete 'pull through' occurred at the bottom corner fixings and the load dropped off in subsequent cycles. There was no uplift of bottom plate from the foundation beam.

1.5.3.2 *PY Specimens W8 & W7 (see also Figure 7)*

@ Displacement mm	Observations
24	The bottom plate had lifted from the foundation beam by 2 mm and the end studs were just beginning to separate from the bottom plate.
36	The two sheets were observed to be rotating separately and the amount of differential movement across the joint was approximately 10 mm. Bottom nails were 'working hard' at this point.
48	During the 48 mm cycles the bottom fixings and centre nail fixings began to withdraw from the framing and nail heads embedded into the linings.
56	There was a drop off in load as several nails along the vertical joint sheared through completely, due to fatigue failure and the bottom plate fixings withdrew from the frame. The bottom plate remained securely attached to the foundation beam whilst the end studs separated from the bottom plate. On completion of the test the loose clouts were removed from the lining and a slight ovaling of the nail hole and crushing of the lining under the nail head was observed. Otherwise the plywood lining was undamaged.

1.5.3.3 *BL Specimens W11 & W12 (see also Figure 7)*

@ Displacement mm	Observations
9	Nails of bottom corners were 'working hard' and began to embed into the paper face.
15	The end stud at end A was seen to be lifting from the bottom plate by approx 6 mm, although no sheet slip was noticeable nor any uplift of the bottom plate from the foundation observed.
23	The bottom corner fixings had experienced complete pulled through. The peak load was recorded at this point
30	Stud uplift increased to approximately 12 mm. No observable movement of the bottom plate had occurred at end A, however the bottom plate was lifting some 5 mm during the reverse cycle at end B.
38	Nail pull-through occurred along each end stud during the tension cycle for a distance of 600 mm up from the bottom plate.

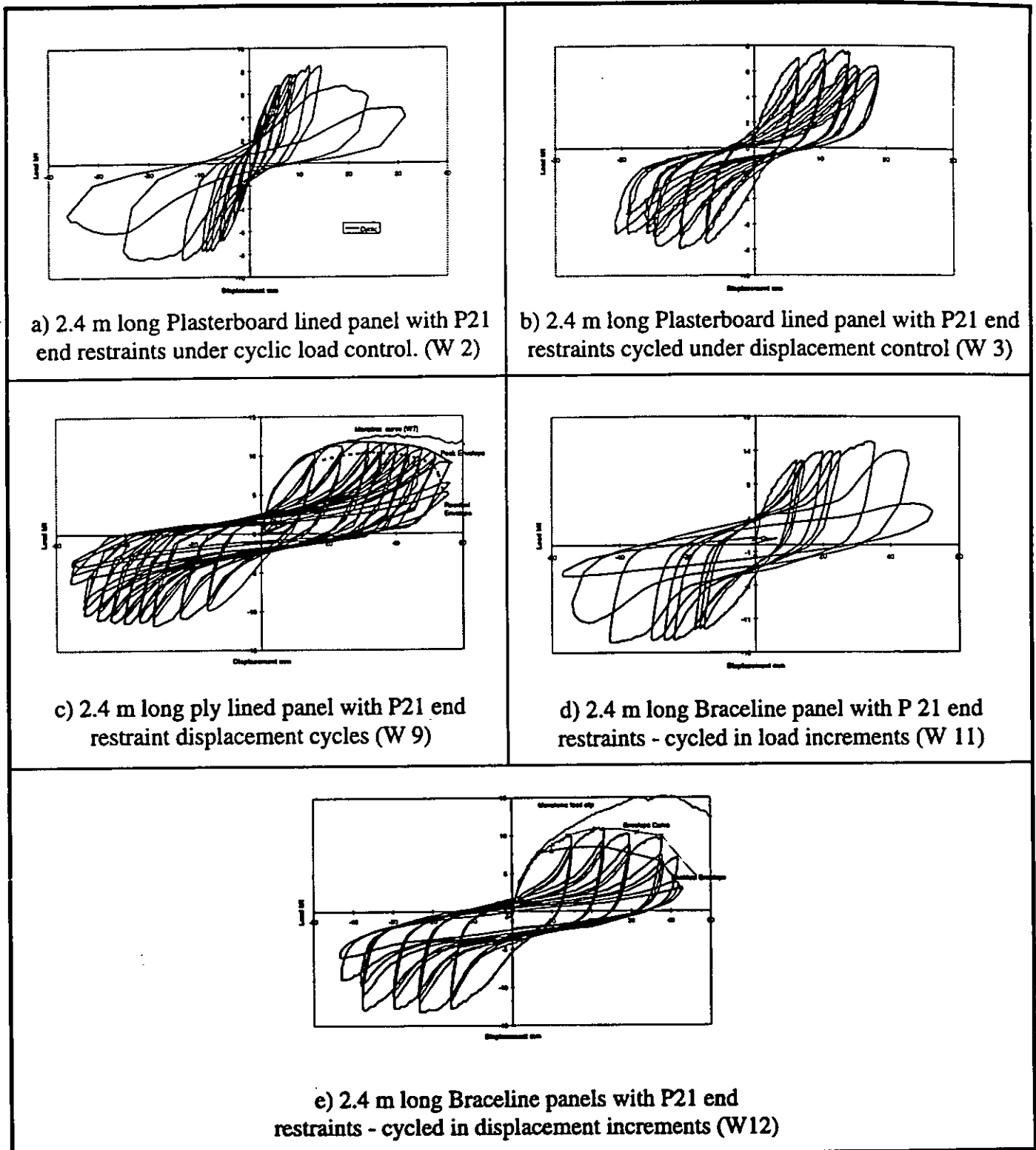


Figure 7 : Cyclic and Monotonic Load Regime for 2.4 m long panels with different linings (Observe that plot scales may differ)

Cyclically loading panels W2, W5, W8 and W11 (which were identical to the panels tested monotonically), produced similar results in each case. The first cycle followed the monotonic curve almost identically. Subsequent cycles to the same displacement showed a load degradation, which was greater between 1st and 2nd cycles than

between subsequent cycles. On the first push beyond the initial displacement (for small displacements at loads less than the peak load) it again reached the monotonic curve. The monotonic curve and the parent curve of the cyclically load test specimens were reasonably well matched up to peak loading. (In all cases specimens under cyclic loading regime did not quite reach the peak loads attained during the monotonic test regime). Cycles beyond the peak load showed an increasingly large variance from the monotonic curve. The variation in load degradation for successive cycles is shown in Figure 8. The plot shows the percentage of load degradation in each cycle from the monotonic curve at various displacements for panel W10 (monotonic) and W12 (cyclic/displacement). Figure 7 graphically shows the effects that cyclic loading has on panels with respect to similar panels subjected to monotonic load only.

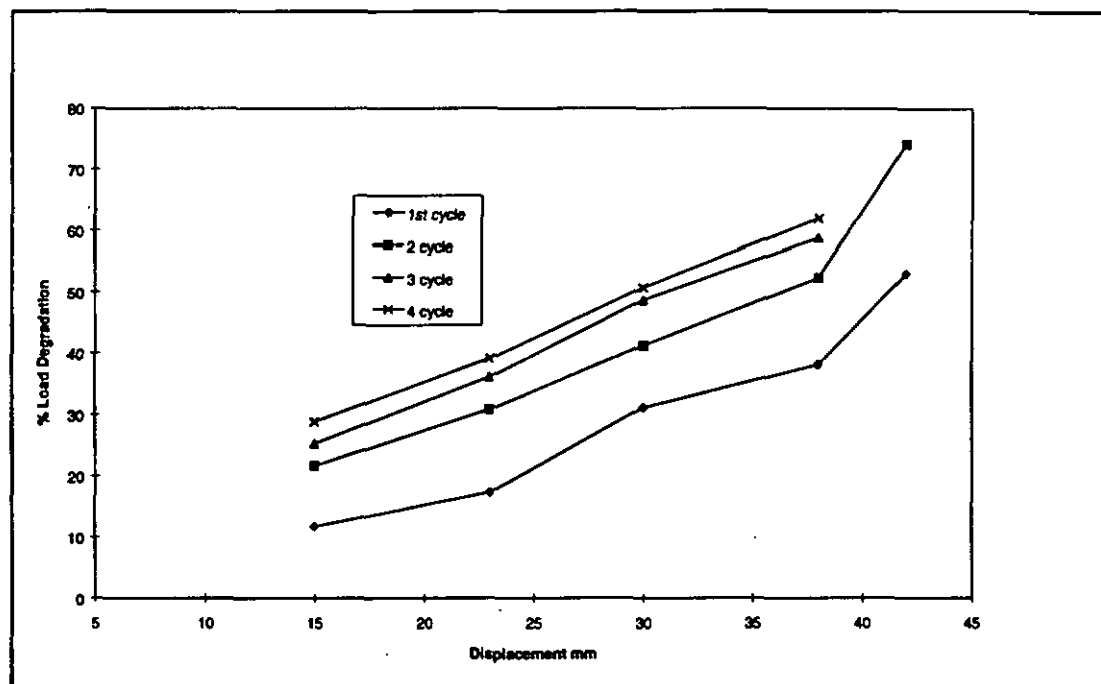


Figure 8 : Percentage Load Degradation from Monotonic Curve (BL) Specimens W10 and W12

There are two features of the test results which are worth highlighting. Both occurred for the load controlled and displacement controlled regimes:

- (i) Little degradation occurs during the cyclic regime at low loads/displacements. Figure 9 shows the displacements at varying percentages of ultimate load (derived from the monotonic test) for 1st to 4th cycles for specimen W6 (plywood and cyclic/disp control). It shows that for loads up to 0.5 of the peak load, little load degradation occurs during cyclic loading. The value of P_u was taken for both the positive and negative cycles. Similar trends were observed for other panels.

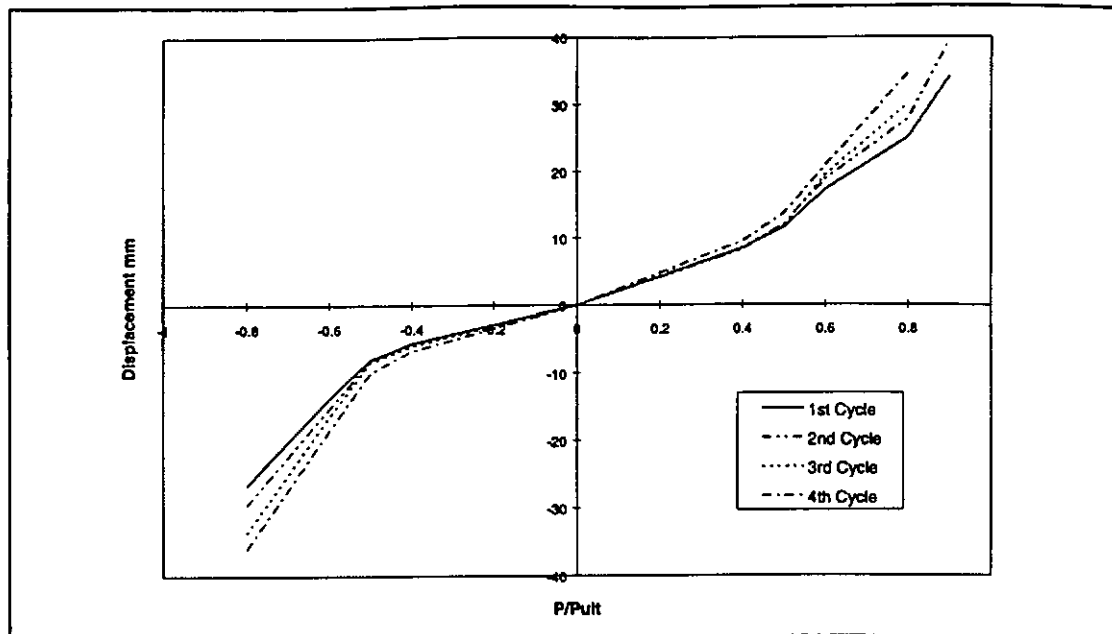


Figure 9 : Displacement at Successive Cycles as a Ratio of Peak Load

- (ii) The residual (ie the displacement at zero load) after each cycle is a function of the maximum displacement of that cycle. Table 4 shows the ratio of maximum displacement to residual displacement for specimens W2 and W5, each of which was tested with P21 end restraints and under cyclic/load control. The results show a reasonably constant ratio for all loading cycles up to peak load.

Panel	Load	Displacement (mm)	Residual (mm)	Disp/Residual
W2 (PB)	0.5 Pu	2.3	0.9	2.5
		2.3	0.8	2.9
		2.4	0.9	2.8
	0.6 Pu	3.3	1.3	2.6
		3.4	1.2	2.8
		3.4	-	-
	0.8 Pu	5.6	2.4	2.4
		6.0	2.4	2.5
		6.2	2.5	2.5
	Max	12.0	6.0	2.0
14.4		7.0	2.1	
W5 (FC)	0.5 Pu	8.4	4.9	1.7
		8.2	3.7	2.2
		8.4	5.0	1.7
	0.6 Pu	17.2	10.5	1.6
		18.8	12.0	1.6
		19.4	12.0	1.6
	0.8 Pu	25.0	16.2	1.5
		27.8	18.9	1.5
		30.1	19.9	1.5
	Max	34.1	23.2	1.5
		39.5	26.0	1.5
		42.7	31.1	1.4

Table 4 : Ratio Of Displacement To Residual Displacement

1.5.4 Cyclic Load and Cyclic Displacement Test Regime Using Various End Restraints

The influence of different supplementary end restraints was investigated by conducting a further three tests on panels identical to W10 (ie bracing grade plasterboard) using different end stud restraints.

1.5.5.1 Tie Rod Restraint Specimens W13 & W16

Displacement mm	Imposed Load kN	Observations Panel W13
8	9	Little damage was observed until the 9 kN cycle when both bottom plate corner fixings began 'working'.
9	10	During the 1st of the 10 kN cycles, all the bottom plate fixings were observed working, with those in the extreme corners 'working hard'.
10	-	During the 2nd cycle the stopped joint fractured at the top of the specimen. The fracture extended down a third of the height of the joint. There was a subsequent drop off in load. There was no apparent 'working' of the end stud fixings. Subsequent cycles saw the nails along the central joint between the sheets working and starting to show through the stopping. Fixings along the top plate were also 'working'.
Displacement mm	Applied Load kN	Observations Panel W16
14	20	Little damage was observed until the 20 kN load cycle, at which time the bottom fixings were 'working'. The sheathing around the both sets of bottom corner nails broke away suddenly.
20	22	Nails along the bottom edge were 'working very hard' and 'nail head pull through' was observed at all corners.
30	24	'Nail head pull through' continued to increase in extent during the 24 kN cycle and the fixings along the centre stud began to 'work.' At this stage no damage was observed along the vertical edges of the panel and the fixings were only 'slightly working' along the top edge.
40+	26	The bottom fixings completely 'pulled through'. Nails along the centre stud up to 300 mm were observed to be 'working hard'.

The load/displacement plot for Panel W13 is shown in Figure 10. The initial stiffness of the panel was higher than the monotonic load curve (using the P21 type end restraint) at approximately 2 kN/mm. Maximum loads on each cycle followed the monotonic curve up to a peak value of 10 kN, at which point there was failure, by nail head pull through along the bottom plate, with a consequential drop off in load carrying capability.

The plot demonstrates the relatively brittle performance of a panel which was restrained from end stud uplift and lined with a degrading material. Some ductility is normally afforded by the partial relaxation of the end restraint, however in this instance, these inelastic deformations were prevented. All the

load was taken through the sheeting fixings into the sheet which degraded rapidly and eventually exhibited a brittle type failure.

It would seem prudent when evaluating this type of panel to assume that it is an elastically responding element and assign it with a structural ductility factor of 1 in accordance with NZS 4203 (SNZ 1992). However, under the current P21 evaluation method (which assigns the on-set of inelastic behaviour to occur at a displacement at which half the maximum load occurs) (King & Lim 1991), specimen W13 would be rated with a yield displacement of approximately 3mm. As the maximum load was at a displacement of 12 mm, the ductility of the panel would be $12/3 = 4$.

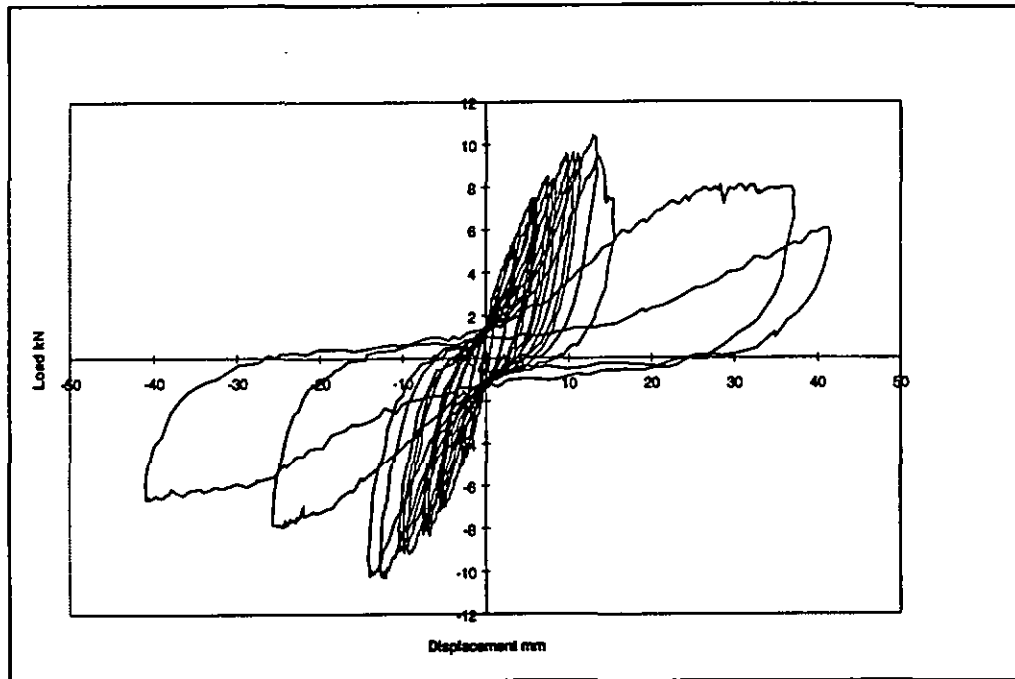


Figure 10 : Hysteresis Loops for Panel W13 - Specimen with Tie-Down Rod Restraint

1.5.5.2 Vertical Load Used as Uplift Restraint Specimen W14

Displacement mm	Applied Load kN	Observations
8	9	There was little uplift of the end stud - approximately 1 mm at the 9 kN cycle.
10	≈10	During the first excursion to 10 kN a majority of the fixings along the bottom plate 'pulled through', however there was little drop off in load carrying capacity.
50		Bottom fixings 'pulled through' the lining completely and the nails along the end studs were 'working very hard' up to 600 mm from the bottom plate.

The load/displacement plot is shown in Figure 11. Up to peak load, the hysteresis loops were similar to those using the tie down restraint. At the peak

load however (≈ 10 kN and 10 mm deflection) there was no drop off in load carrying capacity. Subsequent cycles were able to reach the nearly the same peak load even with large in-elastic deformations. Peak loads of ≈ 10 kN were attained at top plate displacements of between 10 mm and 45 mm, producing stable 'fat' hysteresis loops. A single cycle at approximately 60 mm resulted in a drop off in resistance of around 20%.

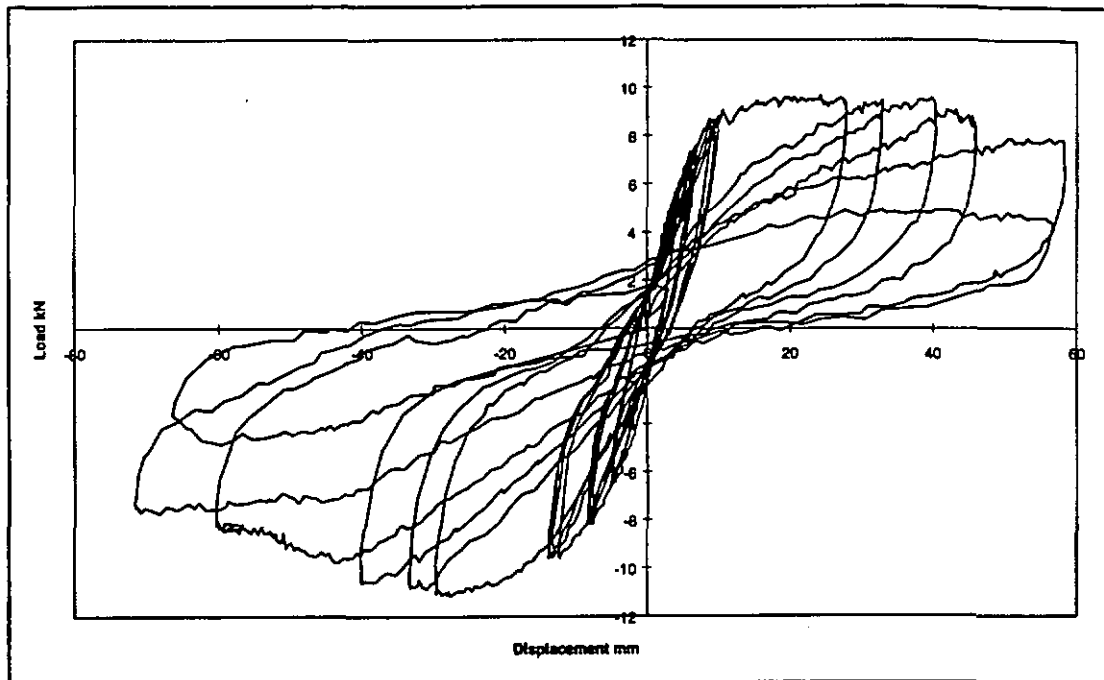


Figure 11 : Hysteresis Plot for Specimen W14 - Vertically Loaded Top Plate

1.5.5.3 No Uplift Restraint Specimen W15

Displacement mm	Applied Load kN	Observations Panel W15
6	6	The bottom plate lifted approximately 3 mm from the foundation beam.
12	≈ 7	The separation increased during the 8 kN cycle with the bottom plate only partially re-seated during the reverse cycles.
25	9	Separation of the bottom plate from the foundation increased until the whole of the bottom plate was 'floating' 10 mm above the foundation beam. There was no observable damage to the linings at the end of the test.

Initial stiffness was lower during the cyclic test than for the monotonic load regime. A peak load of just under 7 kN was attained, and with little reduction sustained over large displacements. Residual displacements were high when compared to other types of end restraint conditions.

1.5.5 Panel W17 (Lintel Specimen)

Displacement mm	Applied Load kN	Observations
6	5	During the 6 mm cycles fixings along the bottom plate were beginning to 'work'. A hairline crack appeared at both lintel joints on line with the outer stud.
16	8	Bottom plate fixings began to 'pull through'. Crack widths at the lintels increased and extended the full depth of the lintel.
24	8	The lintel joints were observed to buckle out of plane and the stopped joint fractured at the junction with the panel sheathing line. There was approximately 10 mm bottom plate uplift and 3 mm separation between stud and bottom plate at end B of the panel. However at end A, the uplifts were 8 mm and zero respectively. The fixings along the top plate over the openings were 'working' but this was not observed to be occurring over the main body of the panel.
36	7	Both lintels buckled out of plane and remained so when the load was removed. The bottom plate was observed to have uplifted 20 mm at end B of the panel but not at all at end A. All the bottom plate fixings had 'pulled through' and fixings 300 mm up the end studs were 'working hard'. There was little drop off in load.
40	7	The top plate fractured at the point where the metal strap diagonal brace was cut into that member (ie a notch type failure of the plate) and the test was terminated.

The nature of the hysteresis loops produced in this test was consistent with the results obtained for panels tested using the standard P21 end restraints. A comparison was made between the uplift restraining force that could be attributed to the P21 end restraint and the effective restraint of the lintel.

Thurston (1993) found that there is a close relationship between the wall racking resistance, P_w , and rigid body rotation displacement, Δw (determined by correcting the system deflection by the panel rotation) obtained during a P21 test. He plotted a number of test results and used best-fit curves matching techniques to develop a relationship between resistance and panel rigid body rotation. For a 1.8 m long wall with no end straps the relationship was given by:

$$P_w = (8.7 \times \Delta w) / (1.3 + \Delta w^{0.95})$$

This is plotted on Fig 11 for rigid body rotation displacements up to 30 mm.

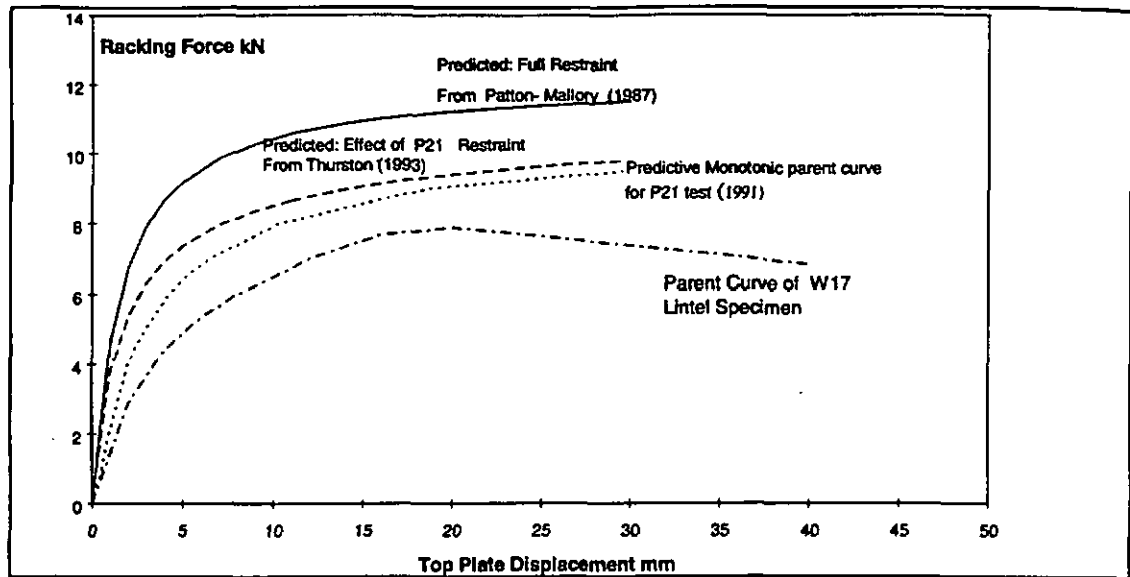


Figure 12 : Predicted Monotonic Parent Curves - Panel W17

The predicted full restraint parent curve shown in Figure 12 was calculated using the theory published by Patton-Mallory and McCutcheon (1987), assuming a panel length of 1.8 m and that the panel was lined both sides with standard 9.5 mm Gib board. Nail slip curves used were those established by numerous past tests carried out at BRANZ. To this was added the parent curve as determined by Thurston (1993) of racking load and rigid body rotation displacement for a standard P21 end restraint with a 1.8 m long panel. The result is the predicted cyclic parent curve for a P21 test on a 1.8 m long panel of height 2.4 m. This curve can be compared to the parent curve of the first cycle of wall W17, (the lintel specimen) and shows the lintel restraint as being less than the P21 restraint.

The amount of restraint required to replicate the lintel can be determined as follows:

From Thurston (1993) the top plate horizontal deflection of say 10 mm due to rigid body rotation on a 1.8 m long panel, using a standard P21 restraint is caused by a racking load P_w of :

$$P_w = (8.7 \times 10) / (1.3 + 10^{0.95}) = 8.5 \text{ kN}$$

From simple statics this corresponds to an uplift force of the end stud

$$= 8.5 \times 2.4 / 1.8 = 11.4 \text{ kN.}$$

From a series of small scale tests (as described in Appendix A) the average uplift capacity of the P21 end restraint was found to be 6.5 kN.

$$\therefore \text{The bottom plate contribution / foundation fixings} = 11.4 - 6.5 \text{ kN} = 4.9 \text{ kN}$$

At the same displacement of 10 mm, the racking force on the lintel specimen is 6 kN i.e. an uplift force on the end stud of $6 \times 2.4 / 1.8 = 8 \text{ kN}$.

The additional restraint required of the end stud over and above that afforded by the bottom plate to foundation fixings is therefore:

$$= 8 - 4.9 = 3.1 \text{ kN}$$

$$\text{i.e. an equivalent of } \frac{3.1}{6.5} \times 3 \text{ (no. nails)} = 1.4 \text{ nails}$$

Therefore it is anticipated that a partial restraint of one or two 3.75 mm ϕ flat head nails would best represent the restraint at door openings. Further testing was carried out in Test Programme II to confirm the restraint required to simulate the lintel.

1.5.6. Description of Light Timber Frame Bracing Panel Hysteretic Behaviour

Figure 7 shows the typical hysteretic behaviour of the lined panels. In the first part of the curve the lining fixings bend elastically and the nail shank crushes the lining material and timber. As the lateral shear load increases the nails deform plastically with the yield point being near the timber/lining shear interface. As deformation continues, axial tension is established within the nail as the nail head bears against the external face of the sheathing. Partial withdrawal of the fixing typically results provided the compressive strength of the lining is sufficient. Alternatively the lining may crush beneath the fastener head. Up until this point, the system is largely elastic and full deformation recovery is usually experienced upon load removal.

With the application of further panel deformation, the nail curvature increases and to maintain nail head/shank geometry, either the nail head becomes embedded into the lining material and /or the fasteners withdraw further from the timber frame. The third possibility of the tension yielding of the fixing is very rare and can be disregarded.

From the onset of inelastic behaviour, when the load is reduced the gradient of the unloading curve is generally similar to that of the initial loading curve.

At zero load there is a residual displacement due to inelastic deformations at the fixings. Loading in the negative direction produces similar hysteresis loops.

During the next cycle to the same displacement, the nail shank is unsupported due to the previous crushing of the lining and timber. Hence the load is resisted by the cantilever action of the nail, with the support point of the nail being at the intersection with the uncrushed timber.

When the panel displacement approaches the previous cycle displacement the nail shank once again becomes supported by the crushed material and there is a corresponding strength and stiffness increase. However, the maximum load on the second cycle does not reach the maximum load of the first.

Subsequent cycles show that the hysteresis curve follows that of the second cycle, with little stiffness degradation. Once displacements reach that of previous cycles the nail shank again bears onto the uncrushed material and there is an increase in strength and stiffness. There is also additional nail withdrawal from the timber. Load increase occurs up to approximately the parent monotonic curve.

Note that no nail withdrawal was observed for Plasterboard (PB), Fibrecement board (FC) or Braceline (BL) linings.

1.6 Conclusions to Experimental Programme Phase I

- The on-set of damage to timber bracing panels lined with degrading sheets can be identified by subjecting test specimens to increasing cyclic displacements.
- There is no significant difference in either the maximum lateral resistance or in the related maximum reliable displacement to which a specimen can attain by adopting a load controlled or displacement controlled load regime.
- Degradation of test specimens is minimal under cyclic loading to loads up to 0.4 of peak load.
- The boundary restraint of a bracing panel which is taped and stopped and which terminates at a return wall can be conservatively replicated by a 12 kN hold down.
- The restraint afforded to a bracing panel terminating at a door opening is less than the current P21 method (King & Lim 1991). It is anticipated that a partial restraint equivalent to 3 kN would be more appropriate.
- The Serviceability Limit State (i.e. the onset of cracking) in the lintel specimen was observed as occurring at a top lateral displacement of 6 mm.
- The ratio of residual displacement after each cycle to the maximum displacement of that cycle is reasonably constant up to peak load.

2. EXPERIMENTAL PROGRAMME PHASE II

Test Programme I indicated that the restraint afforded by door lintels is significantly lower than the P21 end restraint. Further tests were carried out in Phase II to ascertain the extent of this reduction observed in Phase I.

The degree of restraint afforded by taped and stopped wall junctions was also to be greater than that provided by the standard P21 end restraint. A 2.4 m long panel (W24) was tested using additional end stud restraint to simulate this condition and assess its significance.

The results for specimen W24 were eventually added to the results from W17 (lintel specimen) and compared to an equivalent long wall tested by Thurston (1993).

All panels were tested in accordance with the revised test regime described in Section 2.3.

2.1 Objective

This experimental programme was designed to:

- Determine the effect that different lining materials and panel lengths had on the panel resistance rating using P21 end restraint and tie down rods.
- Determine whether the proposed method of simulating in-service boundary conditions was valid for door openings and/or wall junctions.

2.2 Description of Test Specimens

The panel configurations studied are shown in Table 5.

Panel	Lining	Restraint	Length
W18	BL	P21	1.2 m
W19	BL	Tie Rod	1.2 m
W20	PY	P21	1.2 m
W21	PY	Tie Rod	1.2 m
W22	PB + BL*	P21 ¹	1.2 m
W23	PB + PB*	P21 ²	1.8 m
W24	PB + PB*	P21 ³	2.4 m

Table 5 : Test Specimen Configuration

- PB + PB denotes a panel lined both sides with plasterboard etc.
- 1. Standard P21 restraint plus a 25 x 1 mm galv. steel strap used at each end.
- 2. Standard P21 restraint one end. Only 1 No. 100 x 4 FH nail other end.
- 3. Standard P21 restraint one end. 12 kN end restraint other end.

Frame construction and test set-up was as for Phase I and described in section 0. Nailing patterns for the different lining materials was identical to those used in Phase I for each sheathing type.

Panel W22 had two galvanised steel uplift restraining straps fixed to each end stud and to the foundation beam using six 30 x 2.5 nails to both the stud and foundation beam.

Panel W23 had a 25 x 1 mm (nominal) galvanised high tensile steel strap to form a diagonal brace within the main body of the specimen. A comparison could then be made of the observations and results with those of the (isolated) lintel specimen (Panel W17) and the panel tested by Thurston (1993) both of which had a diagonal brace.

2.3 Displacement Protocol

The following loading regime was adopted:

Displacement	No. of cycles
± 8 mm	4
± 15 mm	3
± 20 mm	3
± 25 mm	3
± 5 mm increments	3

Table 6 : Test Load Regime for Test Programme II

2.4 Observations

2.4.1 General

The lining commonly experienced local distortions at the fastener as the imposed displacement increased. The zone of greatest distortion was generally along the bottom plate, particularly at the extreme corners during initial cycles, but progressing along the full extent of the bottom plate and eventually along each end stud.

In the following section the term “nails working” or “working hard” (when distortions were more severe) are used to describe the observation that the nail heads were embedding into the lining material. If a nail head pulled through the sheet, this is referred to as “nail head pull through”.

The following observations were made at the corresponding horizontal top plate displacements. The general description of displacement relates to the horizontal top plate displacement.

The ends of the specimen described as end A or B are shown in Figure 1.

2.4.2 Panel W18 - BL with P21 Restraint

@ Displacement mm	Observations
15	Bottom corner nails began ‘working hard’.
20	During the 1st cycle corner nails began to ‘pull-through’. All bottom fixings were ‘working’. Each tension stud uplift approx 5 mm above foundation.
30	Bottom fixings ‘working hard’. ‘Nail head pull through’ of bottom corner fixings. Top fixings ‘working’.
35	‘Nail head pull through’ of bottom fixings.

2.4.3 Panel W19 - BL with Tie Down Rod Restraint

@ Displacement mm	Observations
0-30	Damage to bottom fixings were similar to Panel W18. Top fixings experienced the same extent of damage as the bottom fixings.
35	End stud fixings began "working hard".
40	Virtually all the top and bottom fixings experienced 'nail head pull through'.
40+	End stud fixings experienced 'nail head pull through' for a length of approx 400 mm from top and bottom plates. Studs experienced significant minor axis flexural deformation.

Comments

Hysteresis loops produced for these panels were very similar. Peak loads resisted were both just under 6 kN at approximately the same displacement of 25 mm. The degradation in load carrying capacity on the 4th cycle was also very similar.

Panel W18 showed some asymmetric performance with the pull cycle being somewhat weaker (ie a peak of 4 kN) than in the push direction.

Maximum reliable displacements for the two panels were both determined to be 25 mm. Initial stiffnesses were 0.8 and 0.6 kN/mm for W18 and W19 respectively.

2.4.4 Panel W20 - PY with P21 Restraint

@ Displacement mm	Observations
15	Bottom corner fixings began 'working'.
20	Bottom plate at end A split at the junction with the nails into the foundation beam, approx 75 mm from the end of the plate. The split extended to the end of the plate.
30	All of the bottom fixings and 300 mm up each end stud were 'working'.
40	Bottom plate split at end B in a similar manner to that which occurred at end A. The bottom plate extreme corner nails had noticeably withdrawn. Stud uplift was measured at 8 mm.
50	Bottom plate nails over 300 mm from each end showed withdrawal. Further splitting of the bottom plate was apparent.

2.4.5 Panel W21- PY with Tie Down Rod Restraint

@ Displacement mm	Observations
	Observations were generally the same as those for panel W 20. Fixings along the top plate behaved in a similar manner to bottom plate fixings throughout the test.
45	By the 45 mm cycles the end studs were observed to be experiencing minor axis flexural deformation, similar to that experienced by Panel W19.
55	On the 55 mm cycles virtually all of the top and bottom plate fixings experienced 'nail head pull through'.

Comments

Both tested panels produce symmetrical hysteresis loops. Peak load for W21 (7.5 kN @ 35 mm) was significantly higher than for W20 (5.5 kN @ 35 mm) indicating that the full tie- down situation is certainly not a lower bound condition.

Maximum reliable displacements were determined to be 35 mm for both panels, (cf 25 mm for panels W18 and W19). Initial stiffnesses for the two panels was 0.5 kN/mm and 0.4 kN/mm respectively.

2.4.6 Panel W22 - PB + BL with end Straps. P21 Restraint

@ Displacement mm	Observations
20	Bottom corner fixings to PB lining began 'working'.
25	Bottom corner fixings to BL lining began 'working'.
30	All of the bottom fixings and 300 mm up each end stud were 'working'. The foundation beam was observed to be lifting from the test rig at end B. This was due to insufficient hold down of the foundation beam to the rig at this point. The uplift was measured as 7 mm on the 30 mm cycle.
35	Bottom corner fixings on both sides were 'working hard'.
40	All bottom corner fixings and bottom fixings to the PB lining experienced 'nail head pull through'. The remainder of the bottom fixings to the BL were 'working very hard'.
45	Damage to the bottom plate fixings was severe, with the first three fixings away from each corner having pulled through on both sides with the remainder free to move within 'slots' formed in both linings, stud uplift was approx 6 mm.
55	The bottom plate split at the junction with the hold down straps and the nails to straps began to withdraw. Hold down straps also began to buckle under compression load.

Comments

The maximum reliable displacement of panel W22 was the greatest recorded for any of the tests undertaken, at 50 mm. This amply demonstrates the greater displacement capacity of shorter length panels when adequately tied to the foundations.

There was a highly asymmetric result due in part to uplift of the foundation beam at end B as noted in the observations. However this would have had little effect on the hysteresis loops produced for loads applied in the push direction.

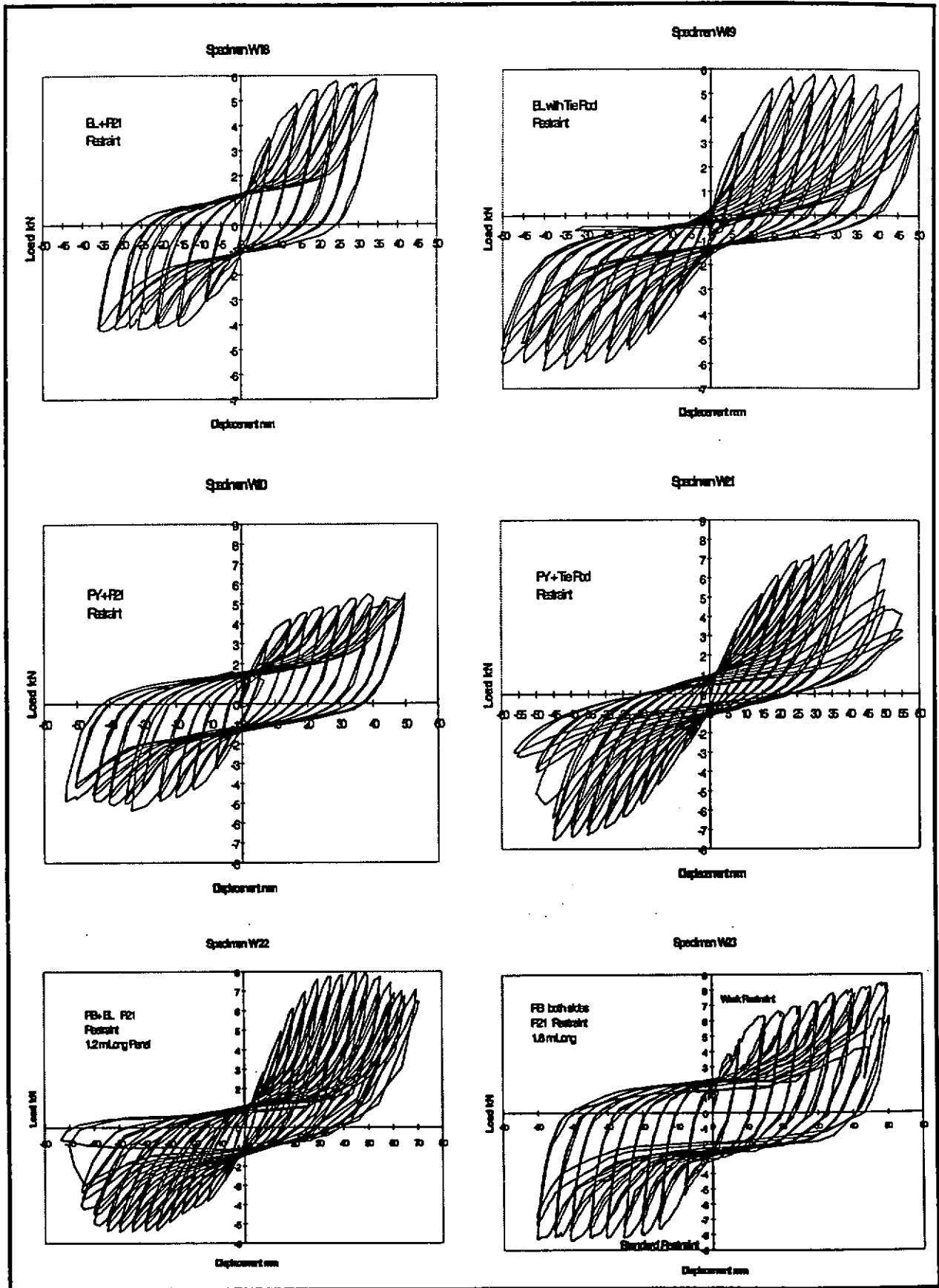


Figure 13 : Hysteresis plots for Specimens W18-W23

2.4.7 Panel W23 - PB Both Sides with P21 Restraint One End and Minimal Restraint the Other

@ Displacement mm	Observations
8	Bottom corner fixings began 'working'.
15	Bottom corner fixings experienced 'nail head pull through'. A split in the bottom plate was observed at the junction with the diagonal strap.
20	The remainder of the bottom fixings were 'working hard'. The end studs were observed to be lifting approx 12 mm from the bottom plate. Racking loads were lower than anticipated and a second 100 x 3.75 FH nail was added to the restraint at end A - making a total of two nails at this end.
25	Bottom plate fixings began to experience 'nail head pull through'. Stud uplift was observed to be 25 mm at end A and 12 mm at end B.
40	Fixings along each end stud began to 'work hard'.
50	All bottom plate fixing experienced 'nail head pull through'. No damage to the top plate fixings were observed.

Comments

The panel exhibited an asymmetric performance due to the different end restraints used. Peak load was not as high as predicted due to splitting of the bottom plate at 8 mm cycles. The peak load on the push cycle, 4.2 kN @ 25 mm (with 1 No. nail restraint) was considerably lower than for the pull cycle, 8 kN @ 40 mm.

An additional nail was added for the 30 mm and subsequent cycles. The effect of this can be seen in the 'step up' in the parent curve at those cycles. The peak loads reached on the push cycle were still less than the pull after the addition of the nail.

2.4.8 Panel W24 - PB Both Sides with P21 Restraint One End and 12 kN Restraint the Other

@ Displacement mm	Observations
8	Bottom corner fixings began 'working hard'.
15	All fixings along the bottom plate were 'working hard'. There was approximately 8 mm uplift at end A (additional restrained end) and 12 mm at end B.
25	Top plate fixings began 'working'. End stud uplift at end A was measured as 6 mm between bottom plate and foundation and 6 mm between bottom plate and stud. The corresponding uplift at end B being 16 mm and 1 mm.
30	The top plate was observed to be moving independently of the frame, with the top plate displacing approx 10 mm more than the top of the end studs. ie the top plate/stud nail shear resistance markedly diminished.
35	The top plate split at the junction with the diagonal brace.

Comments

The results showed a symmetric performance although end A was restrained by six nails.

From section 0 it can be seen that the uplift restraint provided by the standard P21 end restraint on a 2.4 m long panel together with bottom plate nailing was 14.1 kN. This is somewhat lower than the uplift attained in the testing of panel W24 which was approximately 17 kN on a similar boundary restraint. The initial stiffness, k of the panel in the push direction was 3 kN/mm.

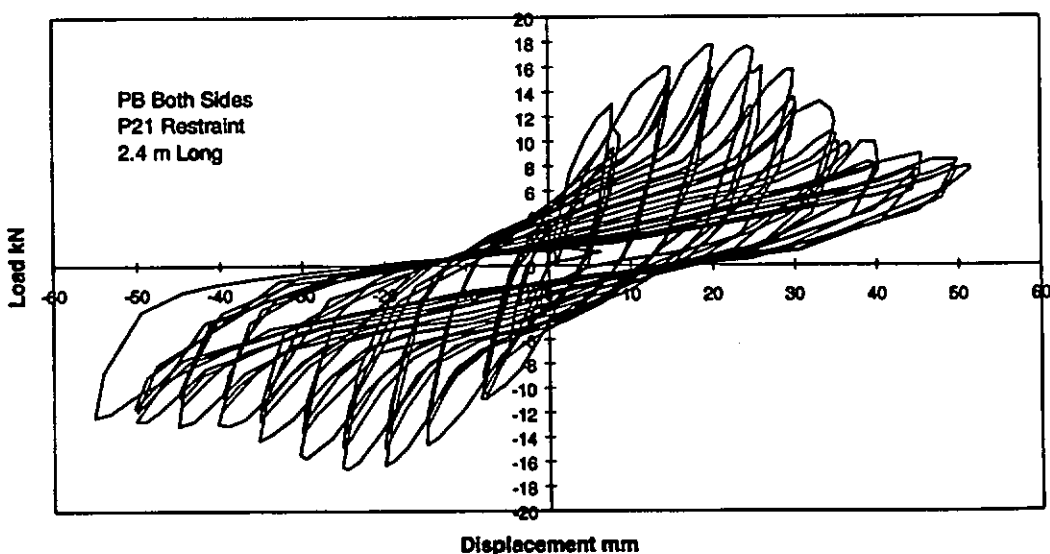


Figure 14 : Hysteresis Loop for Specimen W24

2.5 Summary of Performance Evaluation of Phase II Systems

The results from each panel were analysed using the draft evaluation procedure outlined in Volume 1 Appendix A of this report to ascertain the mass in each case which could be dependably supported by each respective wall bracing panel.

The seismic mass rating procedure outlined in section 3.2 was completed for Test Programme II specimens and the results are shown in Table 7, using the NZA artificial earthquake record at 5% damping.

Panel	Sp. Disp. mm	Stiffness K kN/mm	Period T secs.	Restrained Seismic Mass kg/Panel
W18 <i>BL +</i> <i>P21 Restraint</i>	10	0.8	0.20	770
	20		0.26	1410
	30		0.30	1770
	40		0.33	2200
W19 <i>BL +</i> <i>Tie Rod</i>	10	0.6	0.20	610
	20		0.28	1190
	30		0.32	1540
	40		0.35	1830
W20 <i>PY +</i> <i>P21 Restraint</i>	10	0.5	0.21	530
	20		0.29	1090
	30		0.34	1450
	40		0.38	1850
W21 <i>PY +</i> <i>Tie Rod</i>	10	0.4	0.22	490
	20		0.32	1000
	30		0.39	1540
	40		0.45	2000
W22 <i>PB+BL</i> <i>P21 Restraint</i>	10	0.5	0.20	510
	20		0.30	1140
	30		0.35	1550
	40		0.42	2230
W23 <i>PB+PB</i> <i>P21 Restraint</i>	10	1.4	0.18	1150
	20		0.23	1870
	30		0.27	2580
	40		0.30	3190
W24 <i>Push Cycle</i>	10	3	0.18	2460
	20		0.24	4190
	30		0.27	5530
	40		0.31	7100
	50		0.34	8160

Table 7 : Restrained Masses for Specimens W18-W24

2.6 Comparison of Individual Test Panel Results with Previous Work

Thurston (1993) carried out a series of racking tests on long walls with various window and door openings. He concluded that the actual resistance provided by a bracing panel which terminates at a door opening may be significantly less than those determined by tests when the current P21 end restraint is used (King & Lim 1991). Conversely panels which terminate at a return wall actually experience full hold down restraint.

It is shown in section four that panels which are fully taped and stopped at a return wall have greater restraint than the P21 end restraint and that for timber framed walls on timber foundations this can be replicated by using a 12 kN restraint.

A 2.4 m panel (W24) was tested which had an equivalent 12 kN hold down applied to one of the end studs and the results together with the results of the Lintel Panel (W17) were combined and compared to one of the composite long walls tested by Thurston. (The individual panels W24 and W17 constitute the individual panels which when combined made up Long Wall No. 5 as tested by Thurston).

The Parent curves are shown in Figure 15. When the parent curves of panels W17 and 24 were added together on the push cycle [5] they compared well with the parent curve of the long wall [1]. Parent curves on the pull cycle however grossly over estimated the actual long wall response observed by Thurston (curves 1 versus curve 6). While the lintel response (W17) was symmetric, the degree of restraint provided by the standard P21 restraint (W24) appears considerably in excess of that actually provided by a free ended panel adjacent to the door.

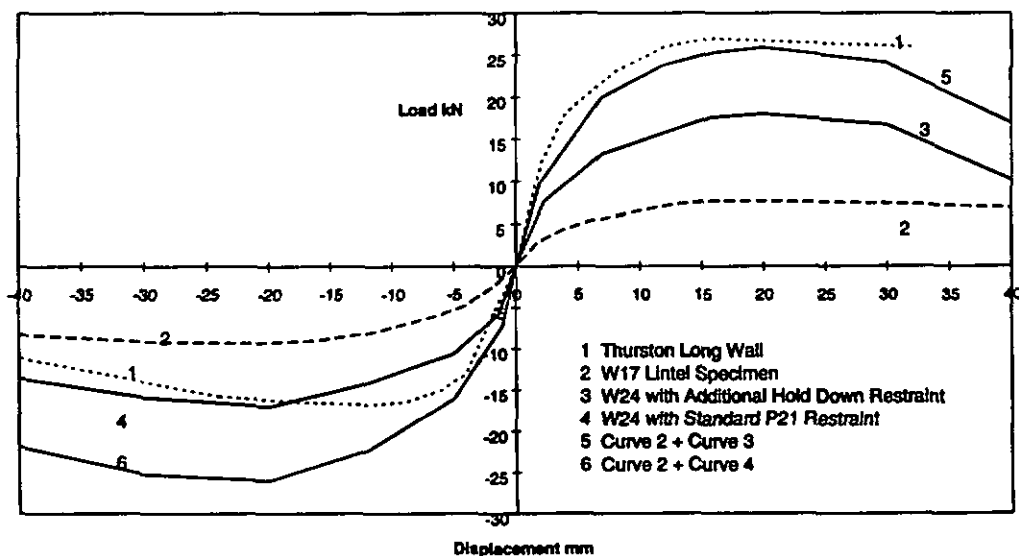


Figure 15 : Comparison of Parent Curves for Lintel and Long Walls

A further comparison was made between the long wall and individual wall components using the draft evaluation procedure (Volume 1 Appendix A). The long wall test hysteresis loops (push cycle only) were matched using the draft analysis procedure prescribed by Phylmas and the restrainable mass at various displacement demands calculated. The results were compared to these obtained on the two

individual panels using the same procedure. Again the earthquake record used was the NZA artificial record and damping was assumed at 5%. The results are given in Table 8. The maximum reliable displacement for the long wall and for Panel W24 were both assessed as 20 mm.

The restrainable mass at displacements greater than the maximum reliable displacement are shown in italics for comparison only.

Thurston Long Wall				Mass restrained by Individual Components		
Sp. Disp. min.	Period T sec.	Stiffness K kN/mm	Mass kg	W24 kg	W17 kg	Total kg
10	.17	5.2	3625	2460	1150	3610
20	.21		6024	4190	1880	6070
30	.24		7700	5533	2400	7930
40	.27		9240	7100	2770	9870
50	.29		11370	8160	3400	11565

Table 8 : Comparison of Restrained Mass for Long Wall Panel

2.7 Conclusions From the Phase II Experimental Programme

- Panel W24 and Panel W17 (which panels combined to match the composite long wall previously tested by Thurston) were tested in isolation. The addition of the parent curves of these two panels showed good agreement with the parent curve of the long wall. The seismic mass evaluated for Panels W17 and W24 when combined was similar to that of the long wall.
- The restraint afforded to a bracing panel by a standard door lintel, and without vertical load, is approximately 3 kN, ie half of that used in the current P21 test procedure.
- The reliable maximum displacement of short bracing panels was greater than for similar panels of longer length provided reliable end restraints can be assured.
- The reliable maximum displacement of short panels having the same lining were similar for both the standard P21 restraint and the tie down rod restraint. The specimen with plywood lining had the greatest displacement capacity.

3. EVALUATION PROCEDURE USED TO DETERMINE THE DEPENDABLE SEISMIC MASS RESTRAINED

3.1 Introduction

The determination of earthquake design actions is covered by Part 4 of NZS 4203 "General Structural Design Requirements and Design Loadings for Buildings" (SNZ.1992). Equivalent-static, modal and integrated time history analysis techniques are all permitted. The equivalent-static design procedure is the most common and easily applied. It is the permitted default for structures less than 15 m in height or when the fundamental response period is less than 0.45 seconds. All structures within the scope of NZS 3604:1990 (SANZ 1990) are therefore eligible to be designed using this technique. The approach requires a lateral force coefficient to be derived for the appropriate ground conditions (three response spectra being published for Rock or very stiff soils, for Intermediate soils and for Soft soils). Each spectra is truncated at 0.45 seconds, although the unmodified elastic response is provided in each case to permit matching for higher mode response effects to be considered. The elastic spectra were derived for a single mass oscillator with 5% critical damping. The inelastic response spectra were derived assuming an elasto-plastic post elastic responding element with equal energy principles being applied over the short period range and equal displacement principle over the long period range (>0.7 seconds).

While the assumed bilinear elasto-plastic post elastic response may be appropriate for many structural materials (eg. well designed reinforced concrete and steel), they are manifestly inappropriate for systems which experience significant degradation during post-elastic excitation. Wall bracing systems used in timber framed buildings are one such degrading system. An alternative model is thus required to represent the inelastic response of these and other systems, which develop slackness. Although the option remains to design such systems to remain elastic at all load levels, this is unrealistic both with regard the cost and real field response. Dowrick (1977) proposed that, provided such systems are designed to ensure they have sufficient inelastic deformation capacity, then collapse mechanisms can be avoided and satisfactory ultimate limit state performance assured. This is consistent with the generally good performance of such systems in the field. (Moss 1992; King 1990; Pender 1987; Cooney 1979).

The essential feature of the evaluation procedure proposed is that the response observed during the experimental phase is matched electronically. The electronic equivalent element then becomes the core of a non-linear time history analysis (Clough and Penzien 1975) using the design spectra from NZS 4203 as the input record. Each period on the resulting response spectra for that element is related to the mass restrained and the elastic spring stiffness of the system. The mass varies with the square of the period. Thus by limiting the mass supported by the structure such that the system displacement does not exceed that which was shown (during the experimental phase) not to induce unacceptable strength loss, then reliable system performance can be assured.

Several researchers have attempted such simulations in the past (Foschi 1977; Stewart 1987; Dolan 1991; Foliente 1993; Dean 1996). Each developed or adopted models which replicated the observed degrading characteristics of the system under consideration. The problem with each was the inability to easily input the elemental parameters to get an adequate response match. Dean (1994) proposed a spring-bar model which provided an encouraging match but suffer the same cumbersome user interface problems previously experienced. This was further refined by Deam (1994) utilising the Microsoft Windows environment to develop a purpose made computer simulation procedure, Phylmas (Pinched Hysteretic Loop Matching and Analysis System) which enables visual matching of the electronic model to that observed experimentally. This approach forms the engine used to undertake the time-history analysis used to generate the displacement response spectra and thence the determination of the maximum lateral mass which can be sustained by the system without exceeding the maximum reliable displacement.

3.2 Seismic Mass Rating Procedure

The following procedure was carried out using the Phylmas programme in determining the seismic mass rating for each of the panels tested.

- (i) The hysteresis loops produced by the test specimen were matched by adjusting the ten generating parameters within the programme.
- (ii) A time history analysis was carried out using each of the following earthquake records (all with 5% damping) and the acceleration and displacement spectra were produced for each using the BRANZ PhylMas software. The analysis methodology is fully described in BRANZ Study Report SR73 - Seismic ratings for Residential Timber Buildings (Deam 1996).
 - (a) An artificial earthquake record NZA was derived by conversion of the design acceleration spectra published in NZS 4203:1992 (SNZ 1992) from the frequency domain into the time domain.
 - (b) The NS component of the 1940 El-Centro earthquake - representative of the acceleration levels found in many of the worlds seismic codes.
 - (c) The NS component of the 1977 Bucharest earthquake - representative of a 'soft soil' with relatively large spectral accelerations and displacements in the one to two second period range.
- (iii) The maximum reliable displacement at which reliable performance can be assured by observation of the test was plotted on the displacement spectra and the natural period T corresponding to this value found.
- (iv) The maximum reliable displacement is the displacement to which the specimen can be cyclically loaded prior to the successive fourth cycle dropping to less than 80 % of the maximum recorded cycle.
- (v) The mass M, able to be restrained by the panel was calculated from the natural period T using the stiffness parameter used in matching the hysteresis loops.

The maximum force and displacement for linear elements subjected to dynamic excitation can be shown (Clough and Penzien 1975) to be a function of the natural period T, which for an elastic element is related to the stiffness k of the element and the restrained mass m by

$$T = 2 \pi \sqrt{\frac{m}{k}} \dots\dots\dots (1)$$

The relationship is normally applied to non-linear elements for convenience even though the period of oscillation varies when there is degradation of the element. The initial stiffness is normally used to estimate k with non-linear elements.

Re-arranging equation (1)

$$\text{Mass } M = \frac{kT^2}{4\pi^2}$$

If Mass M is in Kg, T in secs and k in kN/mm

$$\text{then } M = 25300 kT^2 \quad (2)$$

3.3 Results of Phylmas Analysis for Test Programme I

3.3.1 P21 Restraint

Displacement spectra for tests carried out using the standard P21 end restraint are shown in Figure 16 for specimen W12. The spectra were typical.

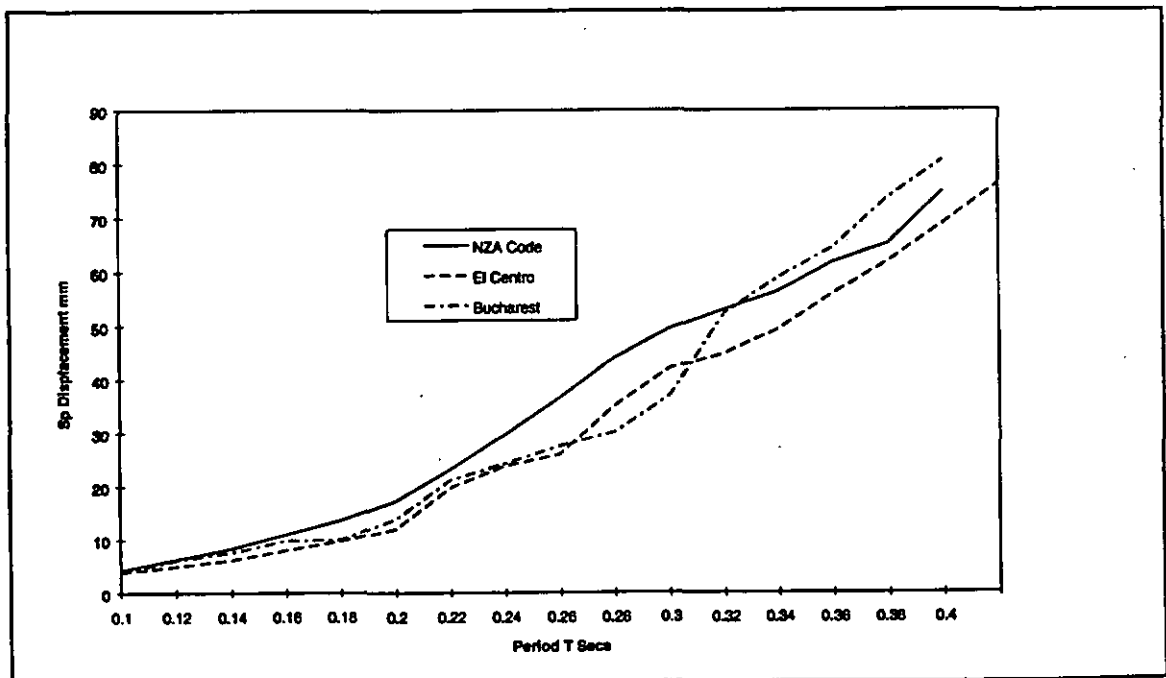


Figure 16 : Displacement Spectra. Specimen W12

Generally the lower bound earthquake record (ie. the record which resulted in the lowest Period T and hence the lowest mass able to be restrained) was the artificial NZA record. This was true for all cases from Period T = 0 secs to approximately T = 0.35 secs when the lower bound earthquake record became the Bucharest 1977

earthquake record. This is not unexpected due to the latter earthquake record being representative of a soft soil site with large spectral accelerations and displacements within the one to two second range.

There was little difference between spectral displacements for earthquake records of Bucharest 1977 and El Centro 1940 up to periods of 0.2 secs.

The validity of results of the time history analysis is dependent upon the characteristics of the earthquake record used. NZS 4203 requires scaling over the period range of interest such that the records match the response spectra of individual events to the uniform risk design spectra. At least three different earthquake records are to be used to provide a representative result.

Spectral accelerations for each of the earthquake records were similar with periods greater than 0.2 secs. Shorter periods showed typically an increase in spectral accelerations for the NZA earthquake record.

3.3.2 NZA Earthquake Record - A Comparison of Spectra

The control earthquake record for all the cyclic/load control tests undertaken using the P21 end restraint was the NZA artificial record.

A comparison of the spectral displacements is given in Figure 16 for specimen W12, and a comparison of mass able to be restrained for each lining using equation (2) at varying reliable displacements is given in Table 9.

The corresponding spectral acceleration and (hence) force is shown for completeness. The initial stiffness k is taken from the appropriate Phylmas generating Parameter.

Panel	Reliable Disp.	Stiffness k , kN/mm	Period T, secs.	Mass Kg	Sp. Accl ⁿ	Force kN
W3 PB	10	2.0	0.15	1140	0.58	6.5
	20		0.19	1830	0.40	7.2
	30		0.22	2450	0.33	7.9
	40		0.24	2910	0.29	8.3
W12 BL	10	2.4	0.15	1400	0.60	8.0
	20		0.21	2650	0.36	9.5
	30		0.24	3500	0.32	11.3
	40		0.27	4390	0.28	12.2
W8 PY	10	1.6	0.16	1540	0.60	9.0
	20		0.22	2730	0.37	9.9
	30		0.26	3400	0.33	11.0
	40		0.29	3940	0.29	11.2
W5 FC	10	2.1	0.18	1720	0.52	8.8
	20		0.24	3060	0.32	9.6
	30		0.27	3870	0.28	10.6
	40		0.30	4780	0.27	12.6

Table 9 : Comparison of Mass Restrained using P21 End Restraint

Note that the masses are those that will cause a panel to displace to the given spectral displacements when subjected to the NZA earthquake. The ability of one lining to undergo larger deformations whilst still resisting load will be reflected in its reliable maximum displacement.

3.3.3 Displacement and Acceleration spectra using various restraints

Displacement and acceleration spectra were produced for Test Panels W12-W15 using the NZA earthquake record and the mass able to be restrained by the panels determined. The results are shown in Table 10. The stiffness k shown in Table 10 is the initial stiffness parameter taken from the Phylmas generating parameter derived at the response matching phase of the Phylmas process.

Panel	Reliable Disp.	Stiffness k, kN/mm	Period T, secs.	Mass Kg	Sp. Acc ⁿ	Force kN
W12 (P21)	10	2.4	0.15	1400	0.60	8.1
	20		0.21	2650	0.36	9.4
	30		0.24	3500	0.32	11.3
	40		0.27	4390	0.28	12.2
W13 (Tie Rod)	10	2.0	0.16	1300	0.6	7.6
	20		0.21	2230	0.40	8.8
	30		0.24	2910	0.35	10.0
	40		0.26	3420	0.31	10.4
W14 (Vert Load)	10	1.6	0.22	1960	0.48	9.2
	20		0.3	3640	0.28	10.0
	30		0.32	4150	0.24	9.8
	40		0.33	4410	0.22	9.5
W15 (unrestrained)	10	1.6	0.18	1310	0.49	6.3
	20		0.23	2140	0.31	6.5
	30		0.25	2530	0.27	6.7
	40		0.27	2950	0.24	6.9

Table 10 : Comparison Of Mass Restrained using Various End Restraints

It can be seen from Table 10 that the mass laterally restrained by the panels using the P21 end restraint is greater than for the corresponding spectral displacements for the tie down rod restraint system. The case which used a vertical load applied to the top plate restrained the greater lateral mass at the lower spectral displacement but was most closely represented by the P21 end restraint condition for displacements up to 40mm.

The unrestrained condition results were always significantly lower than for the other tested panels.

Figure 17 shows the relationship between mass restrained and displacements for each of the end restraint conditions at displacements of 10, 20, 30, 40 and 50 mm.

Note that the masses restrained by the specimen, when subjected to an earthquake record (in this instance the NZA artificial Earthquake record) will displace the specimen to the appropriate spectral displacement. For this purpose the maximum reliable displacements (MRD) have been ignored, hence displacements are shown which are in excess of the MRD.

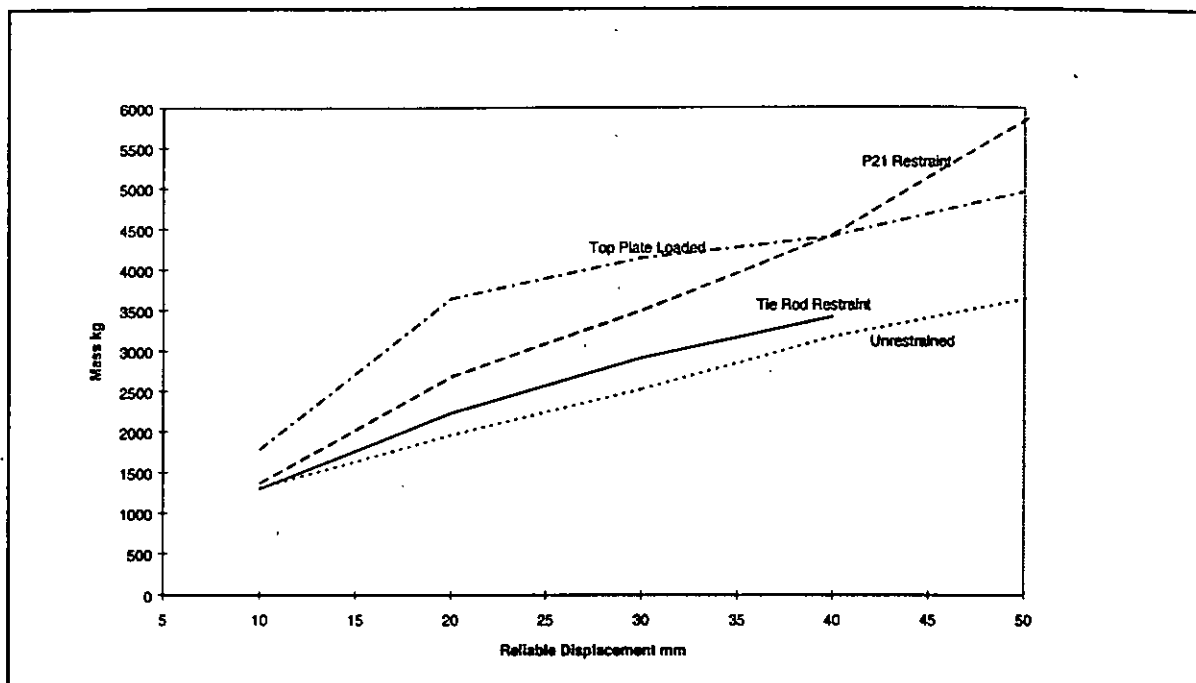


Figure 17 : Mass Restrained using Various End Restraints

3.3.4 Panel W16 - BL Lined Both Sides, Tie Down Rod Restraint

Panel W16 was tested with full restraint of both end studs using the tie down rod system. The test was carried out to investigate the effects of lining a similar panel with the same material on both sides. A comparison could therefore be made with Panel W13. A plot of mass restrained against reliable displacement is shown in Figure 18. The initial stiffness k , of Panel W13 was 2 kN/mm whilst that of Panel W16 was 3.8 kN/mm. Also plotted in Figure 18 is the mass restrained by Panel W13 factored by 1.4.

As part of the background to this study report the effect of initial stiffness on mass restrained using the Phylmas programme has been investigated. One key finding, as might be expected, is that the dependably restrained mass increases with panel stiffness. However, since the panel stiffness is not directly proportional to the panel length, so the dependable restrained lateral mass departs slightly from being linear with panel length. (e.g. Ratio of panels lengths = 2.0 resulting in ratio of restrained mass of 1.9.)

3.3.5 Panel W17 - Lintel Specimen

Displacement and acceleration spectra were produced for the three earthquake records and the lower bound earthquake was found to be the NZA artificial record.

The mass which is able to be restrained by the panel under various reliable maximum displacements was determined and used in the comparison of a long wall tested by Thurston (1993). Refer to section 2.7 for further details.

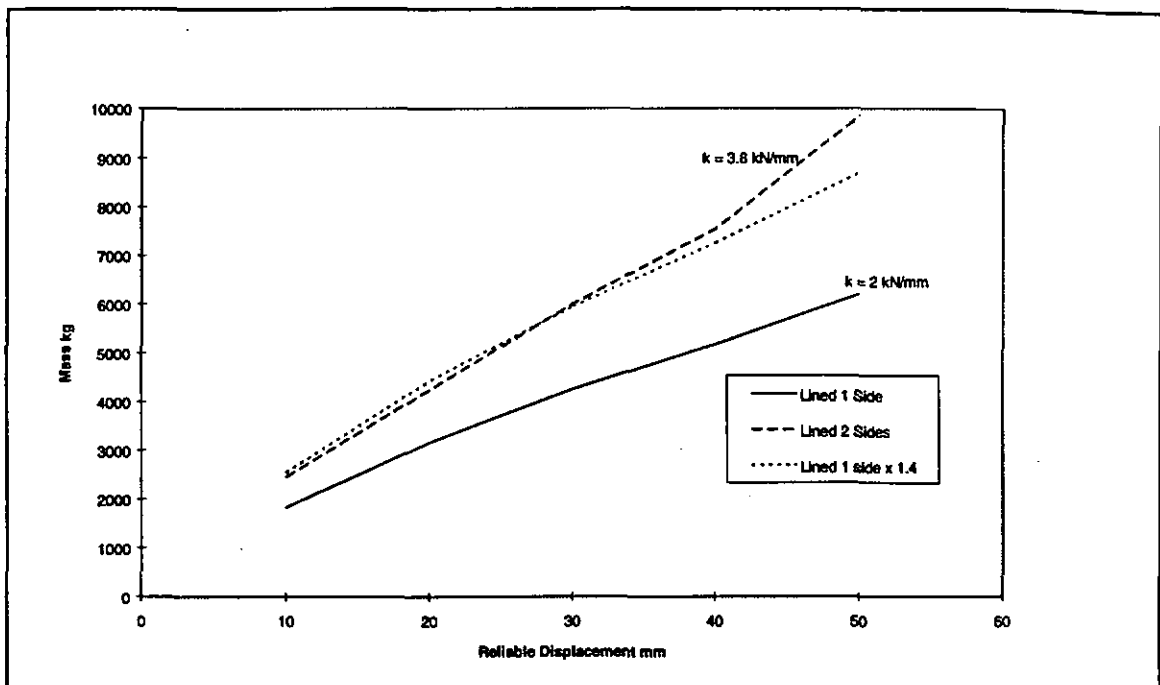


Figure 18 : Mass Restrained by Specimens W13 and W16

4. DISCUSSION

4.1 Boundary Conditions

The seismic mass which a test panel is able to restrain is dependent upon (amongst other things), the initial panel stiffness and the maximum reliable displacement. Both of these are directly affected by the degree of end restraint used to simulate in-service boundary conditions.

The end restraint adopted for the test specimen therefore has a major significance in determining this mass.

The current BRANZ P21 test method specifies that 'appropriate panel end restraint is to be applied'. It gives as an example 'for framed timber, the "P21 end restraint" may be used'. The 'P21 end restraint' referred to is shown in Figure 3 (i.e. an end block nailed to the outer stud with 3 No. 100 x 3.75 flat head nails acting in shear.) This is deemed to be equivalent to the restraint provided to an independent bracing panel when in service (ie as provided by a return wall with cross wall, or by a door or window lintel). Implicit in the method adopted is that the return cross walls are restrained from lifting at loads less than the capacity of the three nails in shear.

In most instances however this method either under or over restrains the specimen for typical cases as described below. As well it does not identify the possible brittle failure of a panel which has sufficient strength to overcome the three nail shear strength by corner gusset action. In this instance the 'ductility' of the specimen could be all attributable to the end restraint rather than the lining material.

4.1.1 Uplift Restraint Attributable to Current P21 (1991) End Restraint

Thurston (1993) evaluated the performance of several test results of P21 tests with P21 type end restraints to establish a relationship between wall racking load, P_w , and wall rocking displacement, Δ_w . The equations he derived for the curves which most closely fitted the results were:

$$1.2 \text{ m long panel} \quad P_w = (5.6 \times \Delta_w) / (3 + \Delta_w^{0.95}) \quad (3)$$

$$1.8 \text{ m long panel} \quad P_w = (8.7 \times \Delta_w) / (1.3 + \Delta_w^{0.85}) \quad (4)$$

$$2.4 \text{ m long panel} \quad P_w = (12.5 \times \Delta_w) / (1.2 + \Delta_w^{0.95}) \quad (5)$$

$$3.0 \text{ m long panel} \quad P_w = (20 \times \Delta_w) / (0.4 + \Delta_w^{0.95}) \quad (6)$$

At 30 mm lateral deflection the wall racking loads are $P_w = 5.9 \text{ kN}$, 9.8 kN , 14.1 kN and 23.3 kN for equations (3) to (6) respectively which corresponds to end stud uplift forces of 11.9 kN , 13 kN , 14.1 kN and 18.6 kN .

The increase in uplift force with wall length can be attributed to the effect of nailing of the bottom plate to the foundation beam.

Small scale tests were carried out to determine the uplift capacities of the 'P21 end restraint', the bottom plate to foundation beam and end stud to bottom plate connections. These are described in Appendix A. The results showed an average uplift resistance of 6.5 kN for the P21 end restraint.

Taking this test result of 6.5 kN and subtracting from the end stud uplift force derived from equations (3) to (6) gives the effect of uplift restraint by the nailing of the bottom plate to foundation for each panel length:

$$1.2 \text{ m panel} = 11.9 - 6.5 = 5.4 \text{ kN}$$

$$1.8 \text{ m panel} = 13.0 - 6.5 = 6.5 \text{ kN}$$

$$2.4 \text{ m panel} = 14.1 - 6.5 = 7.6 \text{ kN}$$

$$3.0 \text{ m panel} = 18.6 - 6.5 = 12.1 \text{ kN}$$

The uplift restraint of the 2.4 m panel compared well to the maximum uplift load of 7 kN attained in specimen W15 which had no end restraints. This showed that the uplift restraint afforded by the P21 end restraint became less dominant with panel lengths greater than 1.8 m .

The lateral shear load transferred across the bottom plate/foundation beam connection was determined analytically as being the top plate lateral load, P_w divided by the number of nails. However several of the nails in the tension zone either reached or approached their withdrawal capacity. If the lateral load carrying capacity of these was zero or reduced then the lateral force/nail is approximately as shown in Table 11. There will be some contribution to lateral resistance by the frictional component between the bottom plate and the foundation at the compression end, however this has been ignored in this simplified analysis.

Panel length m	Max lateral load P_w kN	No. of effective nails	lateral load/nail kN
1.2	5.9	4	1.5
1.8	9.8	6	1.6
2.4	14.1	7	2.0
3.0	23.3	9	2.6

Table 11 : Lateral Force per Bottom Plate Fixing

The ultimate strength of a 3.75 mm diameter nail in single shear, from tests described earlier is 2.17 kN, which suggests that panels of lengths in excess of 2.4 m are governed by the lateral load capacity of the bottom plate/foundation nail connection rather than the P21 end restraint. This is confirmed by Thurston (1993) who plotted the predicted parent curves using full and partial (P21 end) restraint for various wall lengths. He concluded that single lined walls 3 m in length behave in a similar manner for both a fully restrained condition and the P21 end restraint. For walls less than 3 m in length the 'P21 end restraint' effectively governs the wall racking resistance.

Nail slip curves conducted over several years show the maximum lateral force/nail in gypsum plasterboard under cyclic load to be approximately 0.35 kN. If this is translated to a typical 2.4 m x 2.4 m test panel with nail spacing at 150 mm then maximum uplift shear transferred to the end stud can be calculated as the load per nail times the number of nails present (i.e. $0.35 \text{ kN} \left(\frac{2400}{150} + 1 \right) \times 2 \text{ sides} = 12 \text{ kN}$). This is equivalent to the maximum uplift assessed from the P21 end restraint, with the bottom plate nail fixings taken into consideration and as obtained in equation (5). Thus the current P21 (1991) test procedure is optimum for predicting the strength of plasterboard panels whilst down rating panels lined with stiffer, stronger material.

4.2 In-service Boundary Conditions

In order to obtain a realistic bracing rating resistance of a panel experimentally it is important that the boundary conditions used to restrain the panel in the laboratory replicate those that will be found in-service as closely as practical.

4.2.1 Internal Bracing Panel / External Wall Junction

The current (1991) method of end restraint represents the minimum restraint provided by nailing the end stud to the return wall framing. However it does not represent the majority of wall junctions which are, for internal braced walls, usually lined and stopped at the corners, and it makes no allowance for the more direct load path between the lining of the bracing panel and the return wall. The typical wall junction is shown in Figure 19 : Typical Wall Junction

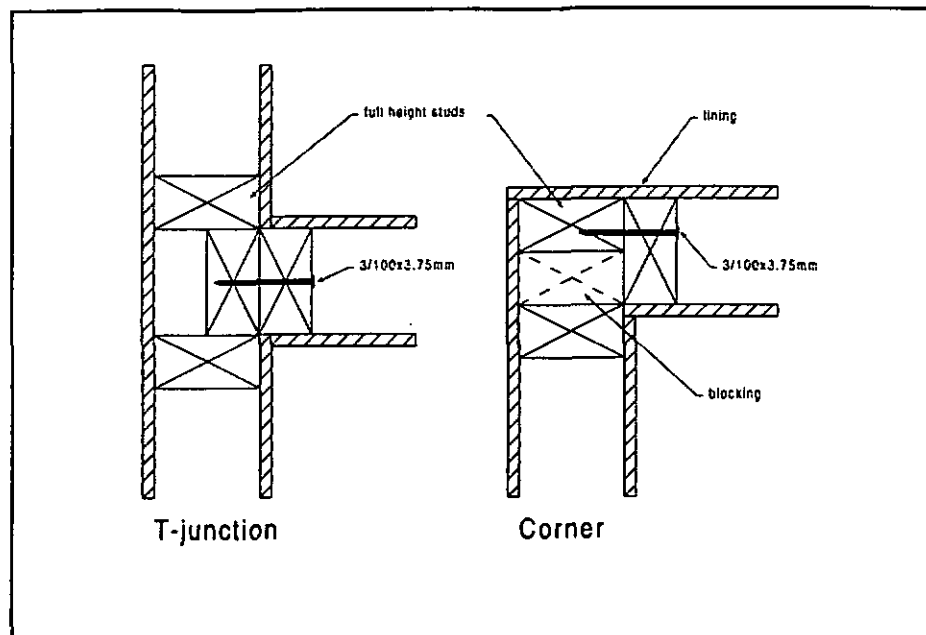


Figure 19 : Typical Wall Junction

4.2.1.1 Stopped Corner Joints

The shear transfer capacity of plasterboard joints which have been taped and stopped has been measured and found to be in the order of 8 kN/m (Thurston 1993). The uplift loads associated with typical bracing panels therefore can easily be transferred to the return wall linings. The uplift force in the panel lining is transferred into the timber studs by a combination of the end brace panel stud nail fasteners and the return wall fasteners.

Nail fasteners in the end stud of the brace wall are subject to load both perpendicular and parallel to the end stud framing.

Referring to Figure 19 it has been found that resistance to uplift of the end stud depends upon:

- (1) The load carrying capacity of the nail fasteners connecting the bottom plate to the foundation, and the return wall length.
- (2) The nail slip characteristics of the lining in the bracing panel, both perpendicular and parallel to the stud.
- (3) The nail slip characteristics of the lining in the return wall parallel to the stud only. This can be determined by small scale testing. The minimum strength joint (ie standard plasterboard lining fixed to the studs using clouts at 300 mm centres) has been found to have a typical nail shear capacity of 0.38 kN for shear applied parallel to the paper bound edge. With nails at 300 mm centres, this results in an uplift capacity contribution of $0.38 \text{ kN} \times (2400/300 + 1) = 3.4 \text{ kN}$. In reality this may be doubled (or more) when the return joint is plastered with uplift forces being passed to the adjacent return panel (refer (5) below).

- (4) The stud to bottom plate connection assumed in section 0 to be 5.4 kN for a 1.2 m long panel. Small scale testing, described in Appendix A, showed the uplift capacity of a pair of 4 mm by 100 mm nails to be 3.8 kN with an additional 50% resulting from uplift of adjacent interconnected panels. (Note that additional restraint afforded by any vertical load on the external wall has been ignored.)
- (5) The shear capacity of the lining joint shear capacity found to be approximately 8 kN/m or 19 kN for a 2.4 m high wall. Such shear transfer is usually subservient to the shear capacity between the sheathing of the adjacent wall and its framing (refer (2) above).
- (6) The extent that the uplifting end stud is connected to the framing of the adjacent return wall (represented in the experimental specimen by the supplementary P21 (1991) end stud uplift restraint shown in figure 3). Small scale testing indicates this restraint to be approximately 6.5 kN (refer Appendix A).

NZS 3604 1990 places no limit on the uplift force which may be imposed on the foundation/floor connections at bracing panels. Similarly the current practice when testing is to assume full foundation beam hold-down is achieved. This is a deficiency of the current system that this revision is attempting to remedy. Appendix B shows that this is excessive for timber framed foundations and a more suitable limit would be 12 kN.

Ideally tests undertaken to determine bracing rating should include the lining joints and return wall to best simulate the in-service condition. However this is not practical. In the case of light timber framed construction, the restraint afforded by return walls can conservatively be taken as being equivalent to 12 kN.

4.2.1.2 Unstopped Corner Joints

In instances where the internal bracing panel is not taped and stopped to the return wall the load path is somewhat different. Uplift forces in such bracing panels are transferred from the sheathing to the end stud of the panel, and then from that end stud into the stud of the adjacent wall by shear transfer through at least three nails. Thence the three nail requirement of the P21 end restraint.

4.2.2 Internal Bracing Panel / Door Opening

Results of the experimental test simulating a panel between door openings (panel W17) is given in section 1.6.4. They show that the uplift restraint afforded by the door lintel is less than that of the P21 end restraint. Hence the use of this particular restraint to simulate the boundary condition over estimates the panel performance. Further testing was carried out in Phase II of this experimental programme to identify the degree of restraint afforded by a door lintel.

4.3 Load Regime

It has been questioned (Dean 1987) whether the P21 test procedure (1991), using a displacement specified regime is adequate to indicate the reserve strength of a test panel or in identifying severely degrading sheets. Dean suggested that a cyclic test to specified loads would be more appropriate.

The current P21 test procedure (1991) nominates a peak displacement and cycles for four excursions to this displacement. No consideration is given to the widely disparate racking performance of different systems beyond that displacement. Some lining material can sustain displacements only slightly higher than that nominated without severe loss of resistance while others can continue to sustain their resistant capacity with only insignificant strength loss. Systems which exhibit this latter response possess both greater ductility and damping and, while being much preferred, are currently given no recognition of this superior performance.

Two means of degrading bracing panels were identified and investigated. The first subjected the test panel to increasing cyclic loads, with a set number four of excursions to each load. Cycling continued at incremental loads until the lateral resistance of the system fell below 80% of the load applied during the previous cycle (i.e. the one preceding the cycle in which significant strength loss occurs).

The alternative subjected the test specimen to increasing cyclic displacements with a set number of excursions to each displacement. The test continued until a maximum dependable displacement was established. The maximum dependable displacement was considered to be the displacement at the cycle immediately preceding that in which the fourth cycle load resistance fell below 20% of the maximum fourth cycle resistant envelope.

In each case the test panel was subjected to cycles beyond the peak load. The onset of significant strength loss is identified.

Phase I of the experimental programme investigated the significance of load regime by subjecting different panels, first to the load regime and then replicate panels to the displacement controlled regime, as shown in Figures 7 and 10 respectively. The on-set of damage in the system is clearly identified in both.

4.3.1 Load or Displacement Control

One objective of this first phase of the experimental programme was to ascertain whether the means of imposing the cyclic deformation influenced the assessed system capacity.

Figure 20 shows the parent curves for both the load controlled and displacement controlled regimes for three types of lining, on similar panels. The close proximity of each envelope indicates that the basis of loading is irrelevant to the assessed performance of the panel. The experimental results have shown that there is no significant difference in the peak load or peak displacements determined using either control regime.

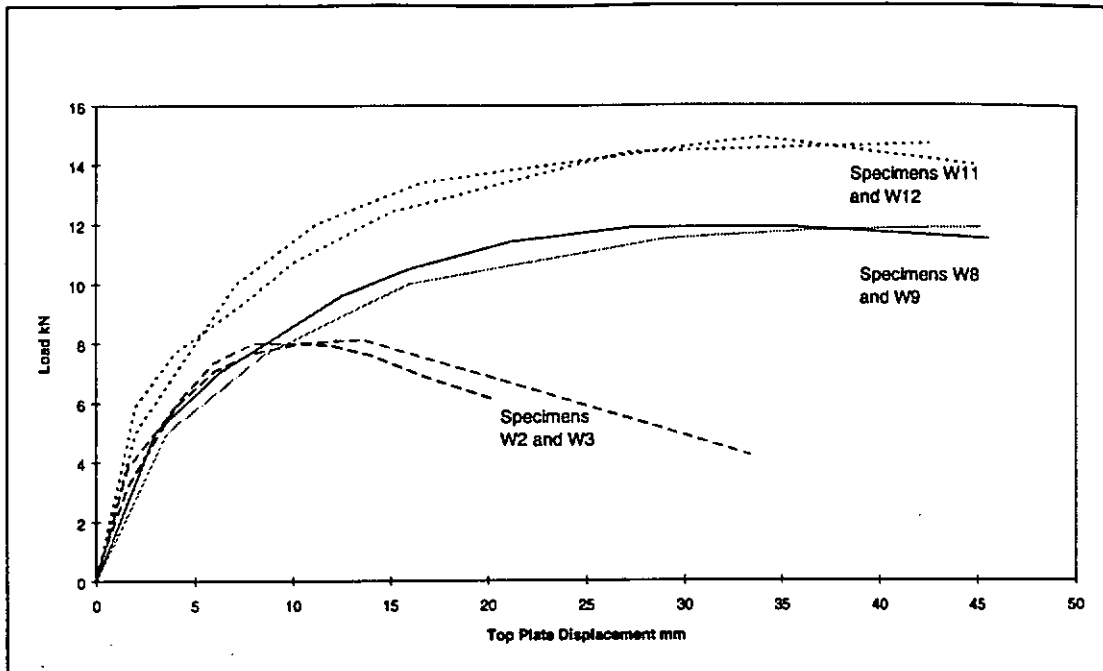


Figure 20 : Parent Curves Under Load or Displacement Control

There are however advantages in using a displacement control method.

- The degree of control provided under displacement control is greater and the system thus safer to operate.
- Displacement cycles are readily matched to the hysteresis loops generated in the Phylmas programme.
- On reaching a particular displacement on the first cycle it is certain that the same displacement can be reached on subsequent cycles. Degradation in the lining may preclude this happening when the test is load controlled.
- Past P21 racking tests and results are based upon displacement control. This may be advantageous when matching test data to the Phylmas programme.

5. CONCLUSION

This report provided the details of the experimental programme undertaken as part of the review process which aimed to rationalise the basis for determining dependable earthquake and wind resistance to bracing panels used in houses.

The necessity of including some allowance for additional bracing panel uplift restraint to reflect actual in-service behaviour was clearly demonstrated and justified. The quantification of the capacity of such experimentally artificial restraint is usually unimportant once a minimum threshold is attained since it will normally be the capacity of the sheathing material itself which controls the inservice performance.

The means or control by which the deformation is imposed has little, if any, relevance to the panel performance since it is the degrading characteristics that need to be matched as input to a suitable time-history analysis technique. The displacement control cycles are thus preferred for experimental simplicity.

REFERENCES

- American Society of Testing and Materials 1976. Standard method for static load test for shear resistance of framed walls for buildings. ASTM E564. Philadelphia.
- American Society of Testing and Materials 1980. Standard methods of conducting strength tests of panels for building construction. ASTM E72. Philadelphia.
- Cooney, R.C & Fookes, A.H.R. 1981. New Zealand houses in earthquakes - What will happen? *In* Large Earthquakes in New Zealand, the Royal Society of New Zealand, Napier, New Zealand.
- Clough, R.W. and Penzien, J. 1975. Dynamics of Structures. McGraw-Hill. New York.
- Deam, B.L. and King, A.B. 1994. The Seismic Behaviour of Timber Structures - A state of the Art Paper. Proc Pacific Timber Engineering Conference. Gold Coast. 1:215-221.
- Deam, B.L. 1997. Equivalent Ductility for Residential Timber Buildings, Building Research Association of New Zealand. Study Report 73. Judgeford.
- Dean, J.A. 1987. The Seismic Strength of Timber Frame Shearwalls Sheathed with Gibraltarboard. Research Report 87/7. Department of Civil Engineering, University of Canterbury. Christchurch.
- Dean, J.A., Stewart, W.G. and Carr, A.J. 1986. The Seismic Behaviour of Plywood Sheathed Shearwalls. Bulletin, New Zealand National Society for Earthquake Engineering 19(1): 48-63.
- Dolan, J.D. 1991. A Numerical Model to Predict the Dynamic Response of Timber Shear Walls. Proceedings, International Timber Engineering Conference, London. 4:338-345.
- Dowrick, D.J. 1977. Earthquake Resistant Design, John Wiley & Sons. Chichester.
- Foliente, G.C., McLain, T.E & Singh, M.P. 1993. A General Hysteresis Model for Wood Structures. Proc. ASCE Congress Structural Engineering in Hazard Mitigation. Irvine. U.S.A., pp 462-267.
- Foschi, R.O. 1977. Analysis of Wood Diaphragms and Trusses Part 1: Diaphragms, Canadian Journal of Civil Engineering, Ottawa. 4(3):345-352.
- King, A.B. 1990. Experiences of Radiata Pine buildings in earthquakes. Proc. International Timber Engineering Conference, Tokyo. pp 962-968.
- Moss, P. J. 1991. The Performance of Low Rise Timber Buildings in New Zealand When Subjected to Seismic, Wind and Snow Loads. *In* Proc. Workshop. Full-Scale Behaviour of Wood Framed Buildings in Watford U.K 1991. North Carolina University, Raleigh, USA.
- Pender, M.J. & Robertson T.W. 1987. Edgecumbe Earthquake - Reconnaissance Report. Bulletin of the New Zealand National Society for Earthquake Engineering, Wellington. Vol 20:3 pp 201-249.

Patton-Mallory M. and McCutcheon, W.J. 1987. Predicting Racking Performance Of Walls Sheathed On Both Sides. *Forest Products Journal*. 37(9): 27-32.

Standards New Zealand (SNZ) 1990. Code of Practice for Light Timber Frame Buildings not Requiring Specific Design, Standards Association of New Zealand, NZS 3604:1990; Wellington.

Standards Association of New Zealand (SANZ) 1984. Code of Practice for General Structural Design and Design Loadings for Buildings. Standards Association of New Zealand. NZS 4203:1984; Wellington.

Standards New Zealand (SNZ) 1992. Code of Practice for General Structural Design and Design Loadings for Buildings. Standards New Zealand. NZS 4203:1992; Wellington.

Stewart, W.G. 1987. The Seismic Design of Plywood Sheathed Shearwalls, Ph.D. Thesis, Department of Civil Engineering. University of Canterbury. Christchurch. 395 pp.

Thurston, S.J. 1993. Report on Racking Resistance of Long Sheathed Timber Framed Walls With Openings, Building Research Association of New Zealand. Study Report 54. Judgeford.

APPENDIX A : SMALL SCALE TESTING OF BRACING PANEL COMPONENTS

Nail pull-out tests were carried out on 10 samples to determine the pull out failure load of the typical bottom plate to timber foundation connection and the failure load of the end stud connection to the bottom plate. Six tests were also carried out on the standard P21 (1991) end restraint to determine the shear capacity.

1. Bottom Plate to end Stud

Two 90 x 3.15 mm gun nails were driven through a 300 mm long section of a bottom plate into the end grain of a 300 mm long 90 x 35 mm timber stud as used in the light timber frames evaluated in experimental phases I and II. The specimen was then assembled into the universal testing machine, with the bottom plate being firmly fixed to the bottom platen and the stud section grasped by the jaws of a vice attached to the machine. The stud was then pulled from the bottom plate at a load rate of 2 kN per minute. Load was measured using a 10 kN load cell. The peak load recorded is shown in Table A.1.

2. Bottom Plate to Foundation

Two 100 x 4 mm bright flat head nails were driven through a section of 90 x 45 mm timber bottom plate, through a 20 mm particleboard strip and into a 150 x 100 mm timber foundation beam. The specimen was then assembled into the universal testing machine with the foundation beam firmly fixed. The simulated bottom plate was firmly gripped and tension load (withdrawal) applied at a rate of 2 kN per minute. Load being measured with a 10 kN load cell. The peak load recorded is given in Table A.2.

3. P21 (1991) End Restraint

Three 100 x 4 mm bright flat head nails were driven through two 90 x 35 mm timber end studs 300 mm long, and were a simulation of the standard P21 (1991) end restraint. The specimens were tested in the universal testing machine with shear load being applied to one of the studs while the other was firmly fixed. The peak load recorded is given in Table A.3.

Specimen	Peak Load kN
1	3.92
2	4.26
3	4.19
4	4.26
5	3.98
Average	4.1

Table : A1

Specimen	Peak Load kN
1	3.45
2	3.94
3	3.62
4	3.63
5	4.22
Average	3.8

Table : A2

Specimen	Peak Load kN
1	6.5
2	6.3
3	6.7
Average	6.5

Table : A3

APPENDIX B : BRACING PANEL UPLIFT ON TYPICAL TIMBER FLOORING

Tests were carried out on a typical house floor to investigate the uplift capabilities at various locations. This may have a direct bearing on bracing ratings, as presently NZS 3604 (SNZ 1990) does not limit the axial load induced in the end studs of bracing panels. There is the possibility of a potential break down in load path from the panel to the foundation.

A 4.4 x 4.4 m square timber flooring system was constructed using 140 x 45 machine stress grade timber joists at 400 mm centres. The ends of the joists were attached to 140 x 45 mm boundary joists. The joists were overlain with 20 mm thick particleboard flooring and all fixings were as specified in NZS 3604. The joists were supported at two locations to provide a joist span of 2.4 m.

Steel straps were firmly coach bolted to the joists at the locations marked 'X' in Figure B1 and load was applied to the straps via an overhead crane. Load was applied until localised failure of the floor occurred. Load was measured using a 100 kN load cell.

Results of the peak load resisted at the various locations are shown in Table B1.

Location	Load At Failure kN	Failure Mode
A	23	Joist fracture
B	20	Joist fracture
C	12	Joist to boundary joist fixing withdrawal
D	14	Joist fracture

Table B1 : Peak failure uplift loads applied to individual floor joists

The results in Table B1 indicate that there is sufficient load sharing within the body of the floor to accommodate the uplift forces generated in the end studs of bracing panel. However, problems may occur at the junction of floor joist and boundary joist where the failure load of 12 kN correlates to a panel bracing rating of 100 Bracing Units for a 2.4 m high wall. Further work is required to verify the significance of this potential failure mechanism.

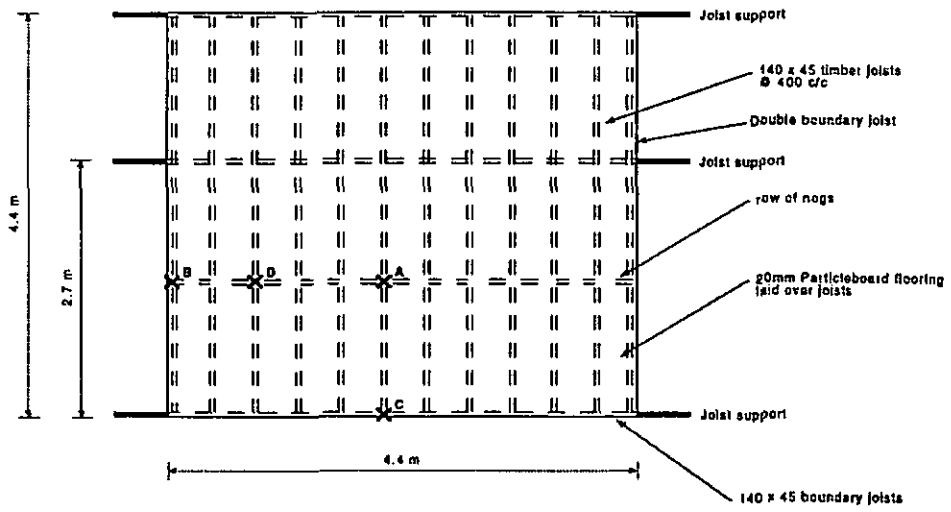


Figure B1 : Experimental procedure used to ascertain load sharing between joists

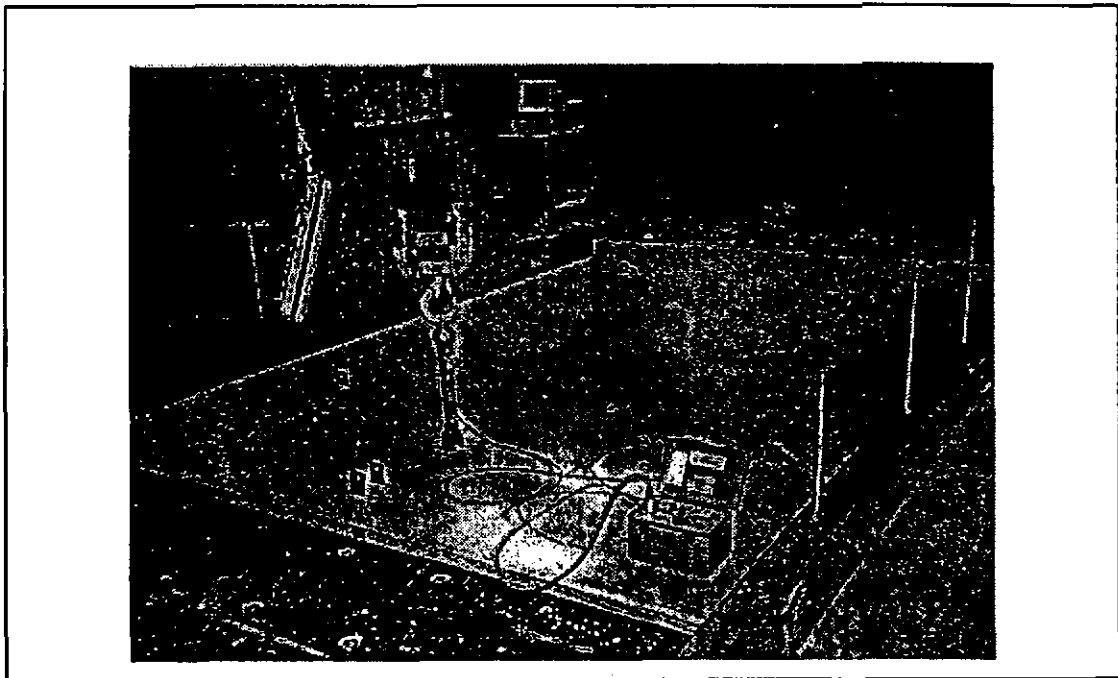


Figure B2 : Vertical load being applied to second joist with load sharing measured



MISSION

To be the leading resource
for the development of the
building and construction industry.

HEAD OFFICE AND LABORATORIES

Moonshine Road, Judgeford
Postal Address – Private Bag 50903, Porirua City
Telephone – (04) 235-7600, Fax – (04) 235-6070
Internet – <http://www.branz.org.nz>
E-mail – postmaster@branz.co.nz

NEW ZEALAND OFFICES

AUCKLAND

Telephone – (09) 303-4902 (900)
Fax – (09) 303-4903
The Building Technology Centre
Victoria Park, 17 Drake Street
PO Box 90524, Auckland Mail Centre

CHRISTCHURCH

Telephone – (03) 366-3435
Fax – (09) 366-8552
GRE Building
79-83 Hereford Street
PO Box 496

AUSTRALIAN OFFICE

Telephone – (00612) 9960 0072
Fax – (00612) 9960 0066
Level 1 Bridgepoint, 3 Brady Street, Mosman, Sydney
PO Box 420, Spit Junction, NSW 2088
